

## **DOPPLER LIDAR FEASIBILITY STUDY FOR THE BALLISTIC WINDS INITIATIVE**

**Michael G. Cheifetz  
David R. Longtin**

**SPARTA, Inc  
24 Hartwell Avenue  
Lexington, MA 02173**

**15 June 1995**

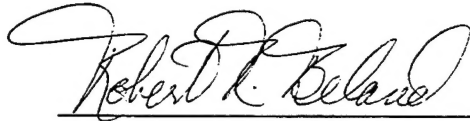
**Final Report  
29 May 1991-31 December 1996**

**Approved for public release; distribution unlimited**

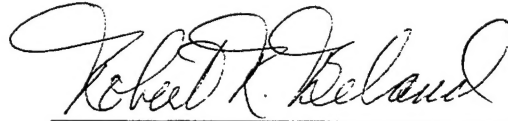


**PHILLIPS LABORATORY  
Directorate of Geophysics  
AIR FORCE MATERIEL COMMAND  
HANSCOM AFB, MA 01731-3010**

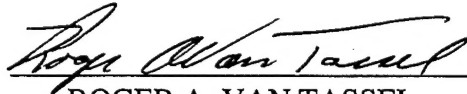
"This technical report has been reviewed and is approved for publication "



ROBERT R. BELAND  
Contract Manager



ROBERT R. BELAND  
Branch Chief



ROGER A. VAN TASSEL  
Division Director

This report has been reviewed by the ESC Public Affairs Office (PA) and is releasable to the National Technical Information Service (NTIS).

Qualified requestors may obtain additional copies from the Defense Technical Information Center (DTIC). All others should apply to the National Technical Information Service (NTIS).

If your address has changed, if you wish to be removed from the mailing list, or if the addressee is no longer employed by your organization, please notify PL/IM, 29 Randolph Road, Hanscom AFB, MA 01730-3010. This will assist us in maintaining a current mailing list.

Do not return copies of this report unless contractual obligations or notices on a specific document requires that it be returned.

REPORT DOCUMENTATION PAGE			Form Approved OMB No. 0704-0188	
Public reporting burden for this collection of information is estimated to average 1 hour per response, including the time for reviewing instructions, searching existing data sources, gathering and maintaining the data needed, and completing and reviewing the collection of information. Send comments regarding this burden estimate or any other aspect of this collection of information, including suggestions for reducing this burden, to Washington Headquarters Services, Directorate for Information Operations and Reports, 1215 Jefferson Davis Highway, Suite 1204, Arlington, VA 22202-4302, and to the Office of Management and Budget, Paperwork Reduction Project (0704-0188), Washington, DC 20503.				
1. AGENCY USE ONLY (Leave blank)		2. REPORT DATE 15 June 1995		3. REPORT TYPE AND DATES COVERED Final (29 May 1991-31 December 1996)
4. TITLE AND SUBTITLE  Doppler Lidar Feasibility Study for the Ballistic Winds Initiative			5. FUNDING NUMBERS  PE 35160F PR 7670 TA15 WUBB F19628-91-C-0093	
6. AUTHOR(S)  Michael G. Cheifetz and David R. Longtin				
7. PERFORMING ORGANIZATION NAME(S) AND ADDRESS(ES)  SPARTA, Inc. 24 Hartwell Avenue Lexington, MA 02173			8. PERFORMING ORGANIZATION REPORT NUMBER  LTR-95-001	
9. SPONSORING / MONITORING AGENCY NAME(S) AND ADDRESS(ES) Phillips Laboratory 29 Randolph Road Hanscom Air Force Base, MA 01731-3010  Contract Manager: Robert Beland/GPOA			10. SPONSORING / MONITORING AGENCY REPORT NUMBER  PL-TR-95-2080	
11. SUPPLEMENTARY NOTES				
12a. DISTRIBUTION / AVAILABILITY STATEMENT  Approved for Public Release; Distribution Unlimited.			12b. DISTRIBUTION CODE	
13. ABSTRACT (Maximum 200 words) <p>The goal of the Ballistic Winds initiative is to improve the accuracy of bomb drops from high altitude aircraft. It has been shown that knowing the vertical wind profile can markedly improve the accuracy of ballistic weapons. As part of the Ballistic Winds Initiative program, the high altitude wind field will be measured with an airborne coherent lidar system. The measurements will then be used by the onboard targeting system to make more refined real time wind corrections. This report investigates the feasibility of obtaining the wind field profile for real time corrections during targeting runs. This study was primarily concerned with obtaining a methodology for predicting the performance of coherent lidar systems which could be used in both the design and field test measurement phases of the Ballistic Winds Initiative Program.</p> <p>The predictions in this report rely on the nominal atmospheres contained within the LOWTRAN models. The expected wind conditions and the atmospheric attenuation and backscatter due to the molecular and aerosol constituents are characterized for mid-latitude spring. The lidar simulation parameters used in the feasibility analysis, which dealt primarily with a 2 <math>\mu</math>m coherent laser, and the signal-to-noise performance relations are described. Lidar performance predictions are given, including range and velocity accuracies, and the utility of pulse integration to improve the signal-to-noise is shown. The wind effects on the aircraft and velocity measurements are also discussed.</p>				
14. SUBJECT TERMS  Approved for Public Release; Distribution Unlimited.			15. NUMBER OF PAGES 34	
			16. PRICE CODE	
17. SECURITY CLASSIFICATION OF REPORT  Unclassified	18. SECURITY CLASSIFICATION OF THIS PAGE  Unclassified	19. SECURITY CLASSIFICATION OF ABSTRACT  Unclassified	20. LIMITATION OF ABSTRACT  SAR	

## Table of Contents

1. INTRODUCTION .....	1
1.1. Background and Purpose of This Study .....	1
1.2. Organization of the Report .....	2
2. ATMOSPHERIC EFFECTS .....	3
2.1. WSMR Wind Field .....	3
2.2. Atmospheric Attenuation .....	3
2.3. Backscatter Coefficients .....	7
2.4. Line-of-Sight Transmission .....	8
3. BALLISTIC WINDS LIDAR SIMULATION METHODOLOGY .....	11
3.1. Ballistic Winds Simulation Parameters .....	11
3.2. Method of Evaluating the SNR Performance .....	12
3.3. Simulation Assumptions .....	12
3.4. Equations in BACKSCAT 4.0 .....	13
4. SNR PERFORMANCE PREDICTIONS .....	14
4.1. Single Pulse Operation .....	14
4.2. Pulse Integration Performance .....	16
4.3. Range and Velocity Resolution Considerations .....	20
4.4. Velocity Accuracy Considerations .....	20
5. WIND EFFECTS ON AIRCRAFT .....	24
6. SUMMARY AND CONCLUSIONS .....	27
7. REFERENCES .....	30

## List of Figures

Figure 1.	Nominal flight path for Ballistic Winds lidar tests.....	2
Figure 2.	WSMR area average monthly wind profiles. ....	4
Figure 3.	Vertical transmission from 12.5 km to 3 km altitude due to molecular absorption. ....	4
Figure 4.	Molecular absorption profiles for mid-latitude atmospheric models. ....	5
Figure 5.	Extinction coefficient profiles for the “peak” laser line. ....	6
Figure 6.	Attenuation coefficient profiles at the “peak” laser line.....	6
Figure 7.	Profiles of the molecular and aerosol backscatter coefficient. ....	7
Figure 8.	Line-of-sight transmission geometry.....	8
Figure 9.	Effect of aircraft cruising altitude on one-way cumulative molecular transmission. ....	9
Figure 11.	Effect of off nadir viewing angle on one-way cumulative molecular transmission. ...	10
Figure 10.	Laser line one-way cumulative seasonal molecular transmission. ....	11
Figure 12.	Molecular attenuation variation effects on BACKSCAT single pulse SNR. ....	14
Figure 13.	Viewing angle variation effects on BACKSCAT single pulse SNR.....	15
Figure 14.	Aircraft altitude variation effects on BACKSCAT single pulse SNR.....	15
Figure 15.	Laser line variation effects on BACKSCAT single pulse SNR. ....	16
Figure 16.	Molecular effects variation on the required number of integrated pulses. ....	17
Figure 17.	Viewing angle variation effects on the required number of integrated pulses. ....	18
Figure 18.	Aircraft altitude variation effects on the required number of integrated pulses. ....	18
Figure 19.	Laser line variation effects on the required number of integrated pulses.....	19
Figure 20.	Required number of integrated pulses to maintain a desired total SNR.....	19
Figure 21.	Velocity accuracy vs. voltage SNR. ....	22
Figure 22.	Viewing angle variation effects on the single hit velocity accuracy. ....	22
Figure 23.	Integrated pulse velocity accuracy vs. altitude. ....	23
Figure 24.	Velocity estimation accuracy for BW Doppler lidar. ....	23
Figure 25.	Aircraft orientation during bomb drop test leg.....	24
Figure 26.	Aircraft heading vs. wind velocity. ....	25
Figure 27.	Off nadir viewing angle effect on LOS wind vector. ....	25
Figure 28.	LOS velocity reduction due to crosswind. ....	26
Figure 29.	Relative LOS horizontal wind component due to lidar off nadir angle.....	27
Figure 30.	SNR improvement factor vs. collection aperture size. ....	28

## **DOPPLER LIDAR FEASIBILITY STUDY FOR THE BALLISTIC WINDS INITIATIVE**

### **1. INTRODUCTION**

#### **1.1. Background and Purpose of This Study**

The goal of the Ballistic Winds (BW) initiative is to improve the accuracy of bomb drops from high altitude aircraft. It has been shown that knowing the vertical wind profile can markedly improve the accuracy of ballistic weapons. As part of the BW program, the high altitude wind field will be measured with an onboard coherent lidar system. The measurements will then be used by the onboard targeting system to make more refined real time wind corrections.

The current study investigates the feasibility of obtaining the wind field profile for real time corrections during targeting runs. This study was primarily concerned with obtaining a methodology for predicting the performance of coherent lidar systems which could be used in both the design and field test measurement phases of the Ballistic Winds Initiative Program.

Some Ballistic Winds field tests are planned to utilize a B-52 aircraft fitted with a Lightwave Laser Inc. tunable Tm:YAG solid state laser Doppler lidar system at a fixed off nadir look angle and locked in a fixed azimuthal direction. The proposed aircraft will fly in a rectangular racetrack flight path at a test range with the bomb drop made in the north-south direction as shown in Figure 1. The tests will occur during the late winter to early spring time-frame. For the White Sands Missile Range (WSMR) test site, this is when there are prevailing westerly winds. The initial bomb drop will use the standard correction procedure using only the aircraft altitude wind speed as input. However, the lidar will take measurements for later analysis.

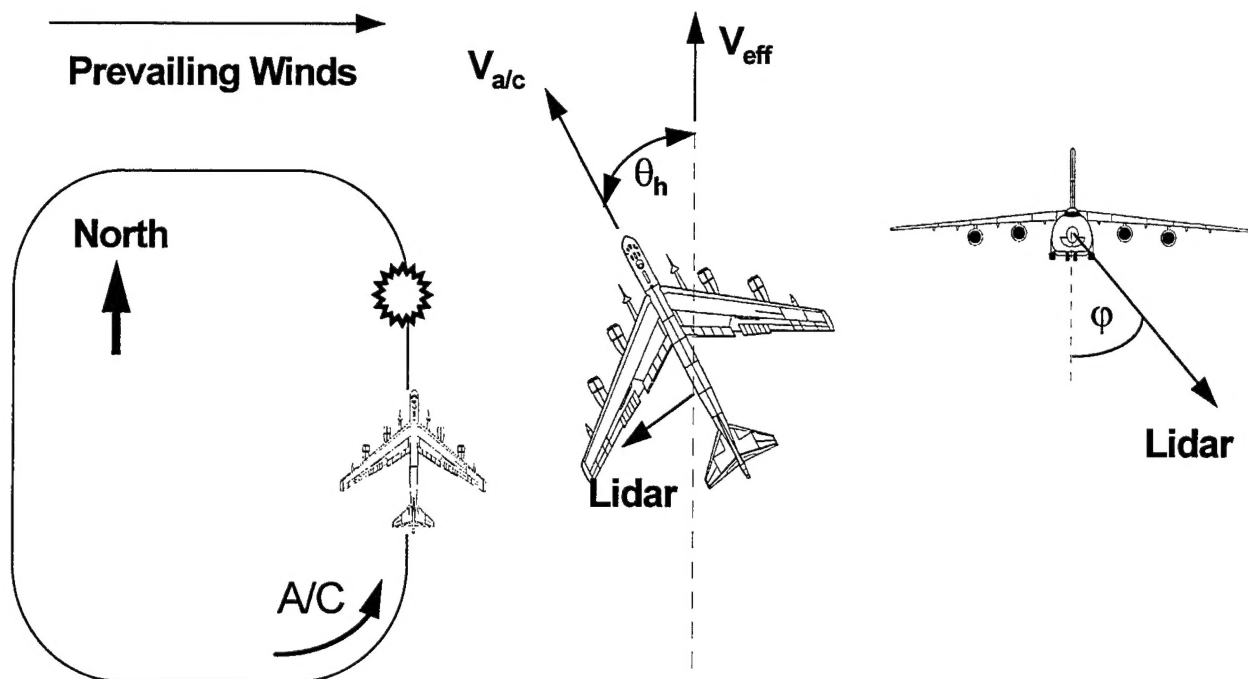


Figure 1. Nominal flight path for Ballistic Winds lidar tests.

## 1.2. Organization of the Report

Section 2 describes state of the atmosphere at a mid-latitude site in spring including expected wind conditions and the atmospheric attenuation and backscatter due to the molecular and aerosol constituents. The atmospheric models including the aerosols, are taken from LOWTRAN7<sup>1</sup> and are only “nominal”, average conditions. They do not give a true representation of actual site conditions and atmospheric measurements should be made at any site planned for BW tests including WSMR. Section 3 describes the lidar simulation parameters used in the feasibility analysis and the signal-to-noise (SNR) performance relations along with the methodology used in the prediction analyses. Section 4 describes the lidar simulation SNR performance predictions. This section includes a discussion of the utility of pulse integration to improve the SNR, and range and velocity error considerations. Section 5 gives a brief discussion of the wind effects on the aircraft and velocity measurements. Summary and conclusions are given in Section 6.

<sup>1</sup> Kneizys, F.X. Shettle, E.P., Abreu, L.W., Chetwynd, J.H., Anderson, G.P., Gallery, W.O., Selby, J.E.A., and Clough, S.A. (1988) *Users Guide to LOWTRAN7*, Air Force Geophysics Laboratory, Hanscom AFB, MA, AFGL-TR-88-0177, ADA 206773.

## 2. ATMOSPHERIC EFFECTS

When evaluating the performance of a lidar system, the state of the atmosphere must be included in the simulation. In analyzing the signal return to the lidar receiver, all the atmospheric effects that degrade and influence system performance must be taken into account. Beam attenuation comes from molecular scattering and absorption, and aerosol absorption and scattering. The aerosol backscatter, which gives the lidar system its return signal, will also be discussed. For a Doppler system, the motion of the aerosols is assumed to be representative of the wind velocity and direction.

The atmospheric conditions assumed for the majority of the analyses done for this study are a mid-latitude spring/summer model with low humidity (40%) in both the boundary layer and troposphere. The model tropopause boundary can vary from 10 to 12 km, depending on the location of the jet stream. Background stratospheric conditions from LOWTRAN7 are assumed. The top of the boundary layer is at 2 km with a 23 km surface visibility and a rural aerosol model. This later region is not important since below 3 km altitude, a bomb is supersonic and crosswinds do not affect its trajectory.

Attention must be paid to the results obtained from a model atmosphere when making system predictions. The results do not always portray the true conditions at a test site and the atmospheric constituents' loadings can vary by orders of magnitude. These variations can greatly affect the conclusions drawn from predictions and care should always be exercised.

### 2.1. WSMR Wind Field

WSMR is just one of the areas being considered for BW field tests. It has limited access and the atmosphere has been measured and characterized. The aircraft will fly at the edge of the jet stream, between 10 and 12 km altitude. At these altitudes, the jet stream winds at WSMR vary between 80 and 120 kts (~41 to 62 m/s). The WSMR area monthly average wind profiles for February through April are shown in Figure 2. These profiles were obtained from an NCAR climatology database<sup>2</sup> for the 1950-1964 time period.

### 2.2. Atmospheric Attenuation

The beam attenuation from molecules at the laser wavelengths of interest is significant. The Lightwave Laser system, a Tm:YAG solid-state laser, is tunable from 2.0133 to 2.0138  $\mu\text{m}$ . Using FASCOD3P,<sup>3</sup> Figure 3 shows the vertical transmission due to absorption covering the tunable laser's wavelength region. The propagation path is from 12.5 to 3 km for mid-latitude

---

<sup>2</sup> Jenne, R.L. (1994) *Jenne's Northern Hemisphere Climatology - Monthly (1950 - 1964) Data Set DS205.0*, NCAR Research Data Archives, Available over the Internet (<ftp://ncardata.ucar.edu/datasets/ds205.0>).

<sup>3</sup> Anderson, G.P., Chetwynd, J.H. (1993) "Fast Atmospheric Signature Code Version 3 - Preliminary", Presented at The Joint Phillips - Wright Laboratories Atmospheric Propagation Workshop, Wright-Patterson AFB, OH, 18 - 20 May, Handout #8.



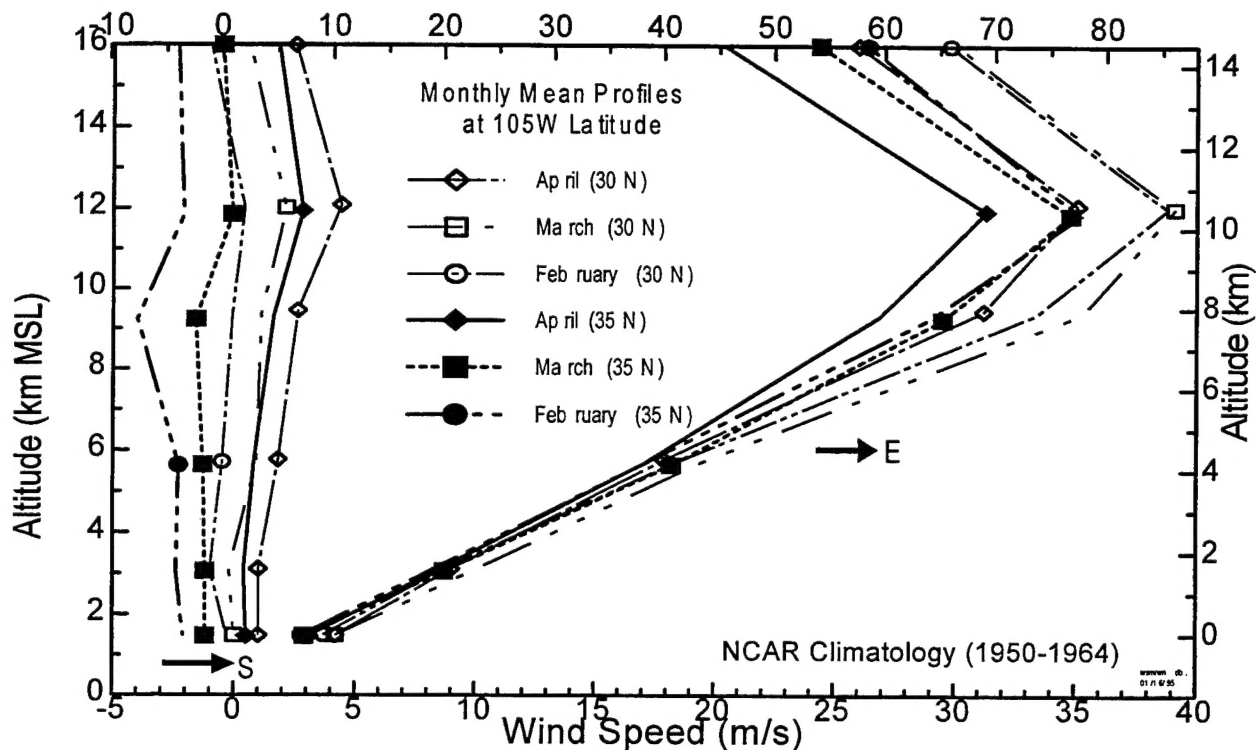


Figure 2. WSMR area (30N - 35N latitude) average monthly wind profiles (1950 - 1964).<sup>2</sup>

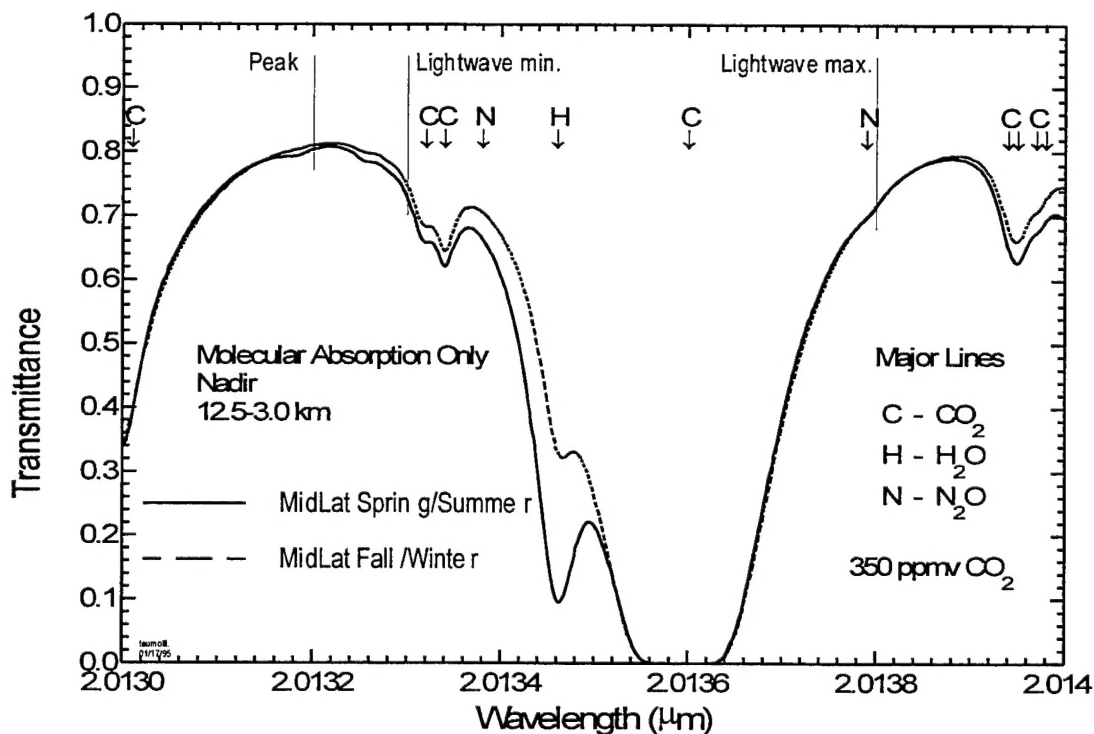


Figure 3. Vertical transmission from 12.5 km to 3 km altitude due to molecular absorption. This is for propagation within the 2.0130 to 2.0140  $\mu\text{m}$  region.

spring and fall conditions. The curve also shows the locations of the major molecular absorbers ( $\text{CO}_2$ ,  $\text{H}_2\text{O}$ , and  $\text{N}_2\text{O}$ ). The minimum wavelength of the Lightwave Laser system (*i.e.*, 2.0133  $\mu\text{m}$ ) is near the peak of the transmission curve (2.0132  $\mu\text{m}$ ).

In this study, future references to the "peak" line refer to 2.0132  $\mu\text{m}$ , while the "off peak" line refers to the best atmospheric transmission (2.0133  $\mu\text{m}$ ) for the Lightwave Laser system.

The molecular absorption profiles for the "peak" and "off peak" laser lines are shown in Figure 4 for typical mid-latitude atmospheres. These values were obtained from FASCOD3P. The sharp increase in molecular absorption below 3 km is due to the water vapor continuum.

The extinction coefficient profiles for the "peak" laser line are shown in Figure 5. The aerosol component is based on the standard Geophysics Laboratory models<sup>4</sup> and the other atmospheric conditions defined previously. The total extinction is due almost entirely to molecular effects. At high altitudes, the molecular extinction is over two orders of magnitude greater than that due to aerosols. Molecular attenuation is due primarily to absorption as shown in Figure 6.

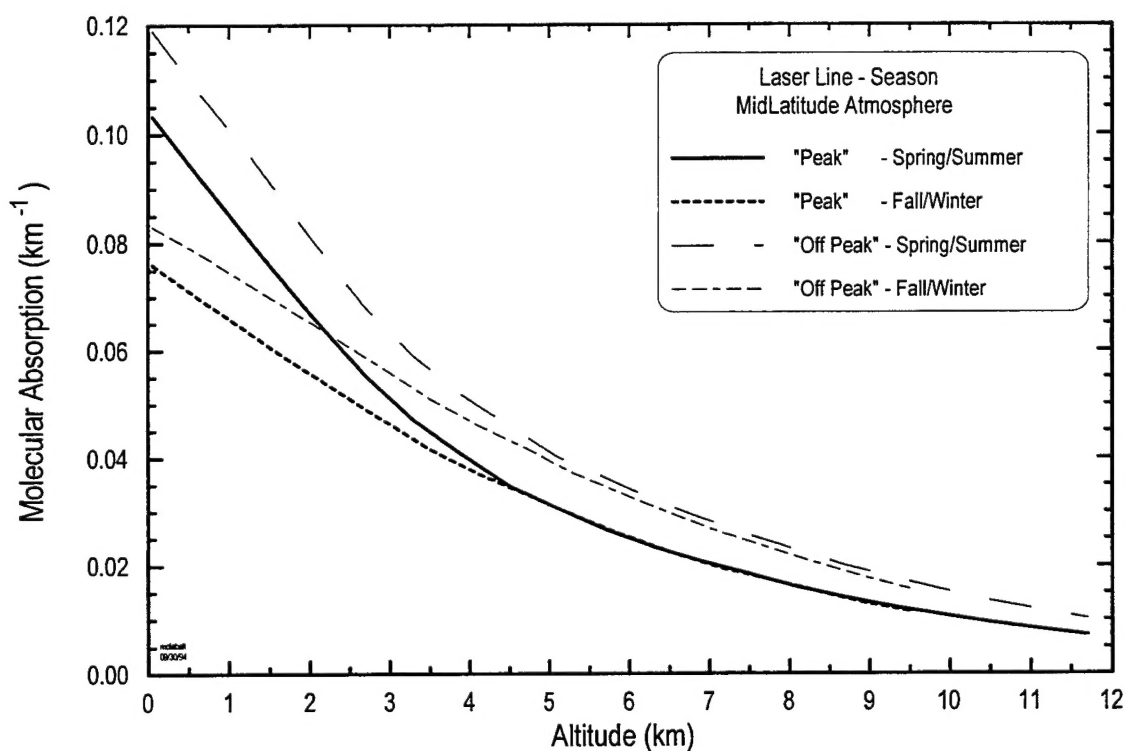


Figure 4. Molecular absorption profiles for mid-latitude atmospheric models. These profiles are for "peak" and "off peak" laser lines.

<sup>4</sup> Fenn, R.W., Clough, S.A., Gallery, W.O., Goode, R.E., Kneizys, F.X., Mill, J.D., Rothman, L.S., Shettle, E.P., and Volz, F.E. (1985) "Optical and Infrared Properties of the Atmosphere", Chap 18 in *Handbook of Geophysics and the Space Environment*, A.S. Jursa (Scientific Editor), Air Force Geophysics Laboratory, Hanscom AFB, MA, AFGL-TR-85-0315, ADA 167000.

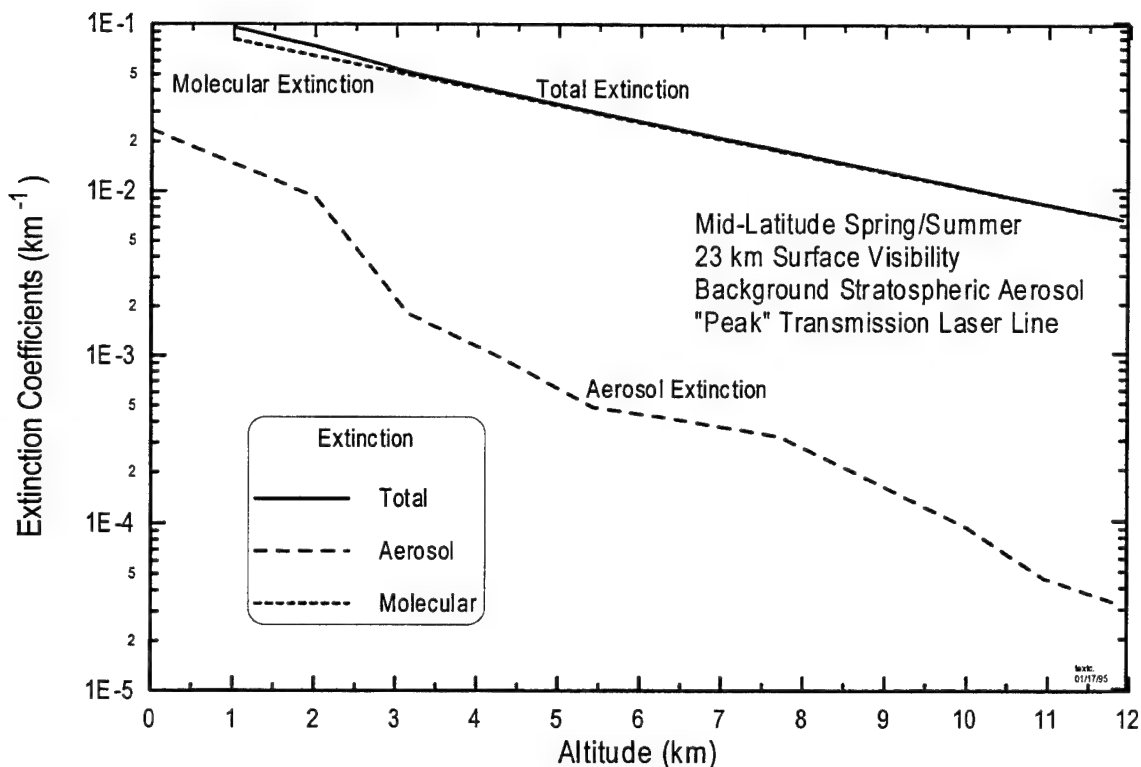


Figure 5. Extinction coefficient profiles for the "peak" laser line.

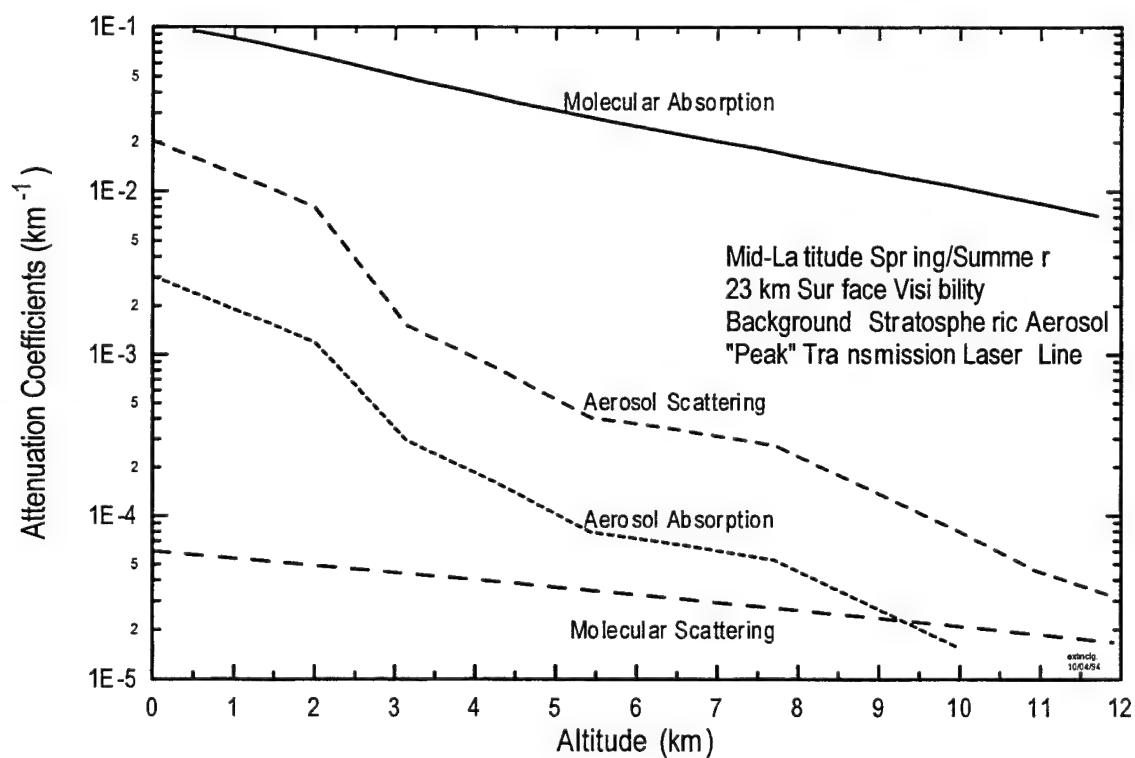


Figure 6. Attenuation coefficient profiles at the "peak" laser line.

### 2.3. Backscatter Coefficients

The profiles of the aerosol and molecular backscatter coefficients are shown in Figure 7. These profiles are valid over the entire wavelength region of interest. The molecular backscatter can only further degrade the velocity measurements.<sup>5</sup> There is significant contributions to the backscatter coefficient at short wavelengths from molecules. This effect can mask any base velocity due to winds. Because the molecules are traveling randomly with a mean velocity near the speed of sound, the energy returned from the backscattered molecules is randomly spread over a wide Doppler spectrum with little energy within each velocity bin. Therefore, the Doppler shift from these molecules cannot be used to estimate wind velocity. In the signal-to-noise calculations, which will be discussed later, molecular extinction due to both absorption and scattering is included, but the backscatter for the coherent system only includes the aerosol backscatter signal. It will therefore have little effect on the system signal-to-noise.

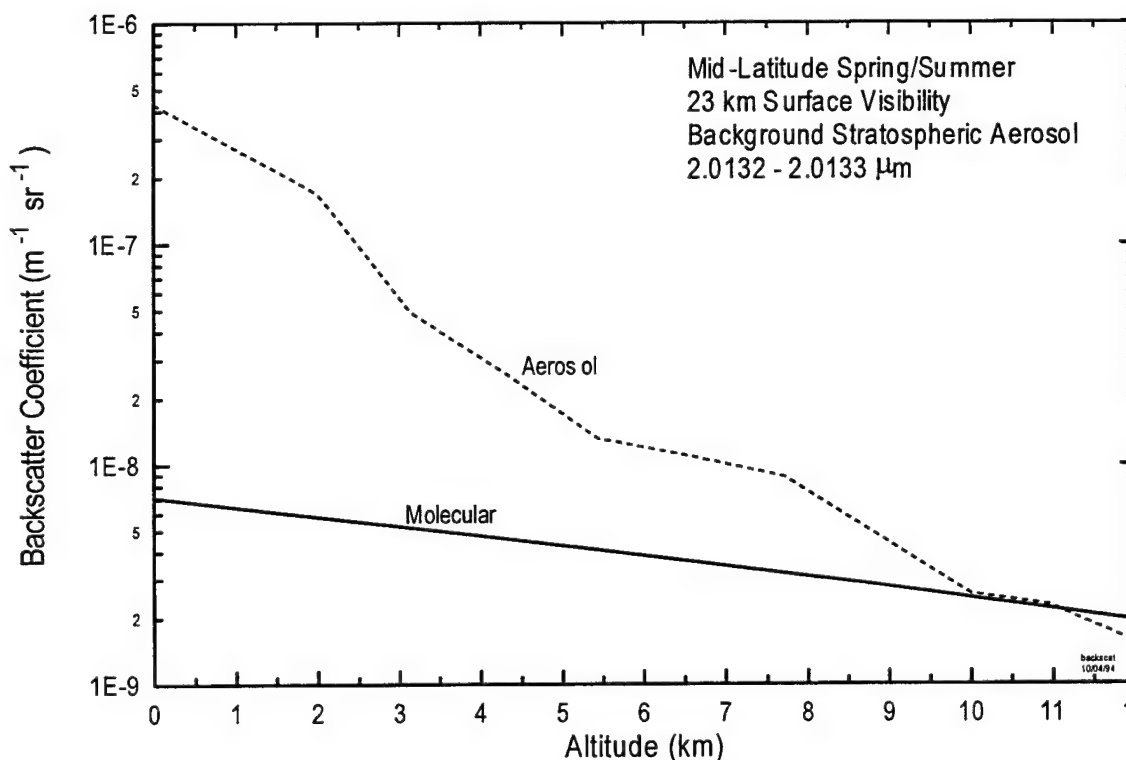


Figure 7. Profiles of the molecular and aerosol backscatter coefficient.

<sup>5</sup> S.E. Moody (1987) "Evaluation of Laser Technologies for On-Aircraft Wind Shear Detection," SPIE Vol. 783, p.124.

## 2.4. Line-of-Sight Transmission

The line-of-sight (LOS) transmission losses can be calculated within BACKSCAT 4.0<sup>6</sup> and LOWTRAN7, but simplified transmission calculations were made to quickly get a sense of the variation due to altitude, season, viewing angle, and laser line. The relations between the extinction coefficient and the vertical distance traversed make use of the geometry shown in Figure 8.

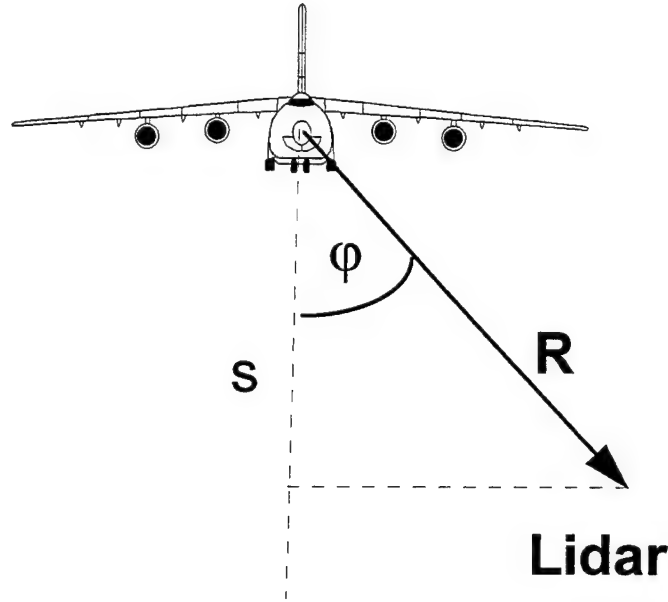


Figure 8. Line-of-sight transmission geometry.

The vertical transmission ( $\tau_v$ ) is defined as

$$\tau_v = \exp \left( - \int_{h_2}^{h_1} \alpha(s) ds \right), \quad (1)$$

where  $\alpha$  is the extinction coefficient and  $s$  is altitude. Thus, the LOS transmission ( $\tau$ ) is,

---

<sup>6</sup> Longtin, D.R., Cheifetz, M.G., Jones, J.R., and Hummel, J.R. (1994) *BACKSCAT Lidar Simulation Version 4.0: Technical Documentation and Users Guide*, Phillips Laboratory, Directorate of Geophysics, Hanscom AFB, MA, PL-TR-94-2170, ADA285851.

$$\begin{aligned}
\tau &= \exp \left( - \int_{R_2}^{R_1} \alpha(R) dR \right), \\
&\approx \exp \left( - \int_{h_2}^{h_1} \alpha(s) \sec \varphi_N ds \right), \\
&\approx \tau_v^{\sec \varphi_N}.
\end{aligned} \tag{2}$$

The expressions in Eq. (2) are approximate because a plane-parallel atmosphere is assumed.

The "peak" laser line one-way cumulative molecular transmission at 30° off nadir shown in Figure 9 for three different aircraft cruising altitudes. By 3 km altitude, there is not much difference between the cumulative transmissions, less than 2%. The off nadir viewing angle variation for the "peak" laser line with aircraft altitudes of 12 km and 10 km is shown in Figure 11. Figure 10 shows the effect of season on the cumulative molecular transmission for the "peak" and "off peak" laser lines. Although there are considerable losses of up to 44%, the variations shown on individual figures are not large.

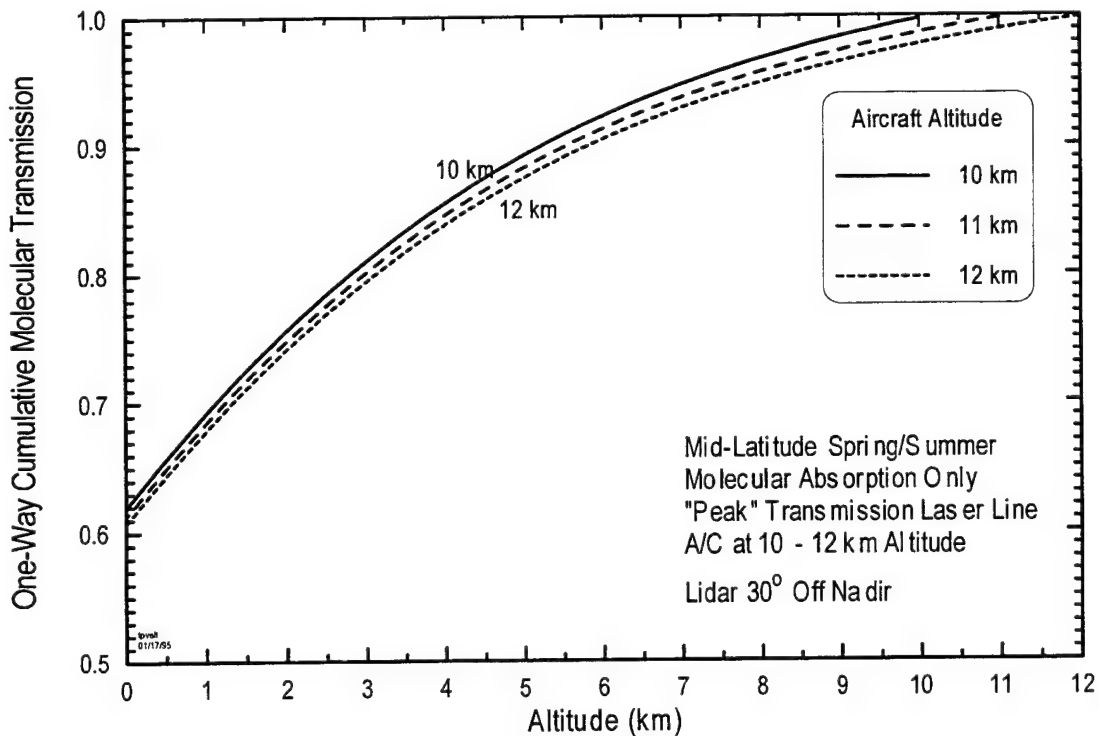
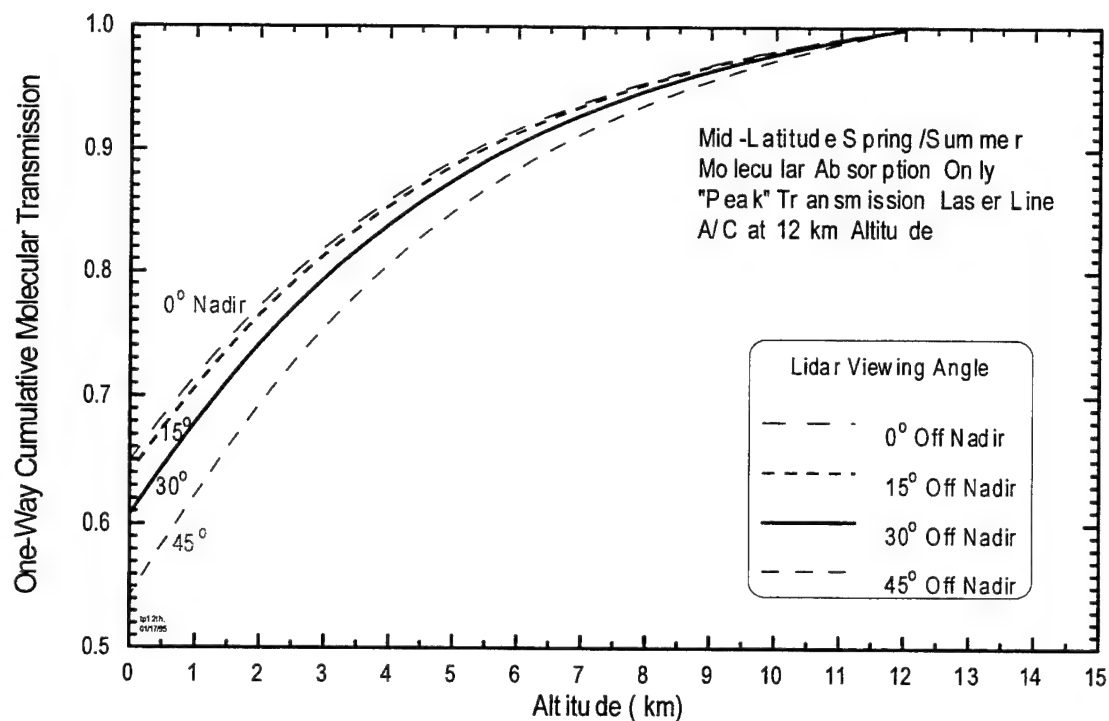
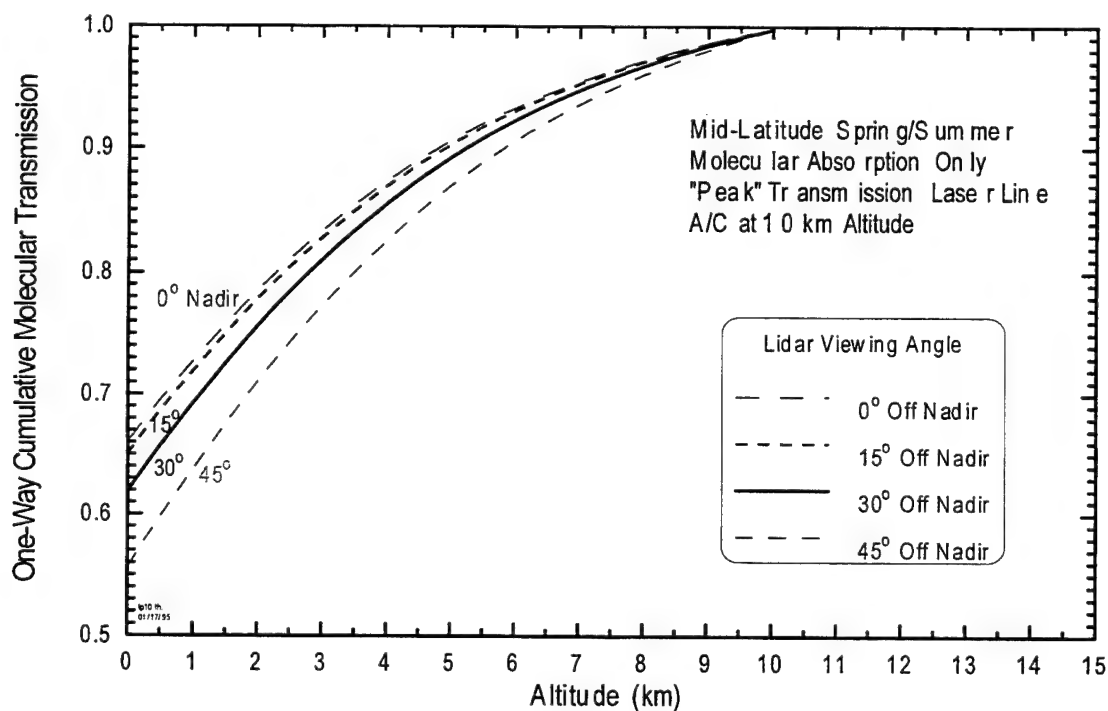


Figure 9. Effect of aircraft cruising altitude on one-way cumulative molecular transmission. These transmission profiles are for the "peak" laser line only.



(a)



(b)

Figure 10. Effect of off nadir viewing angle on one-way cumulative molecular transmission. These are for the "peak" laser line from aircraft altitudes of (a) 12 km and (b) 10 km.

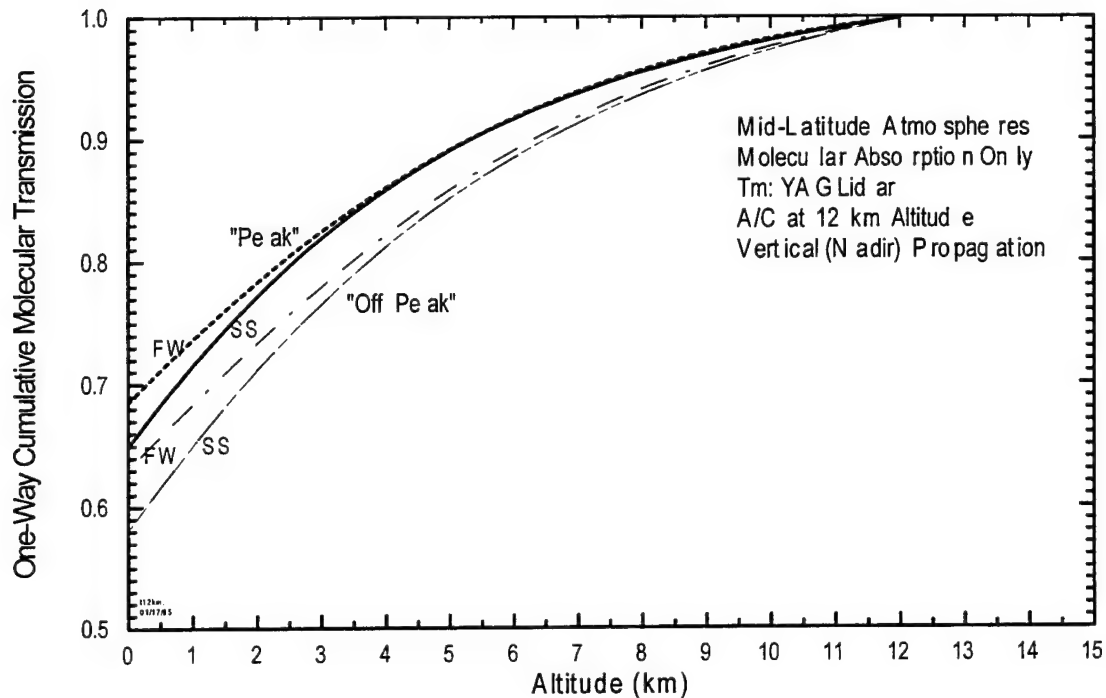


Figure 11. Laser line one-way cumulative seasonal molecular transmission. These profiles are for "peak" and "off peak" laser line transmissions. FW = fall/winter, SS = spring/summer.

### 3. BALLISTIC WINDS LIDAR SIMULATION METHODOLOGY

#### 3.1. Ballistic Winds Simulation Parameters

This section describes the system and simulation parameters used in the performance study. The parameters deal with the laser transmitter, the optics, and the receiver/detector values. The B-52 aircraft flies between 10 and 12 km altitude above the ground with a speed of 220 to 225 m/s. The lidar is fixed at an off nadir viewing angle of either 30° or most likely 15° due to mounting and viewing limitations in the aircraft fuselage.

The Lightwave Laser system laser transmitter has the following specifications -

1. Tunable solid-state Tm:YAG
2. Wavelength:  $\lambda = 2.0133 \mu\text{m}$  ("off peak") to  $2.0138 \mu\text{m}$ , "peak" laser line of  $2.0132 \mu\text{m}$  also used
3. Pulse energy:  $E_p = 3 \text{ mJ}$
4. Pulse length:  $t_p = 0.25 \mu\text{s}$
5. Pulse repetition frequency (PRF):  $\nu = 180 \text{ Hz}$



The laser/aircraft optics has the following parameters -

1. Aperture diameter: 7 cm
2. Overall lidar optical efficiency (two-way, transmit & receive):  $\tau_T \tau_R = 10\%$
3. A/C quartz window transmission (two-way):  $\tau_w^2 = 94\%$

The receiver/detector parameters are -

1. APD detector: EPITAXX 100T GR 2.2
2. Quantum efficiency:  $\eta = 61\%$
3. Excess noise factor:  $F = 1.2$
4. Detector system bandwidth:  $B = 2 \text{ MHz}$ .

### 3.2. Method of Evaluating the SNR Performance

The SNR performance predictions were made using BACKSCAT Version 4.0 in the pulsed coherent Doppler lidar simulation mode. The molecular absorption was included by independently running FASCOD3P, creating absorption profiles, and then inputting them into BACKSCAT. The molecular backscatter was not included in the return power, although attenuation due to molecular scattering was included. The user defined detector option is used for the EPITAXX avalanche photodiode (APD). The outputs from BACKSCAT used in this study are:

1. the lidar return vs. altitude and range,
2. the single pulse SNR (voltage) vs. altitude and range, and
3. the velocity and range accuracy vs. altitude and range.

BACKSCAT runs were used to predict the single pulse signal-to-noise performance of a coherent Doppler lidar system looking towards the ground from the aircraft. Variations in molecular attenuation, lidar viewing angle, A/C altitude, and laser line propagation were considered. The amount of pulse summing required to increase the  $\text{SNR}_p$  to 10 dB was examined. The results of these calculations will be discussed in Section 4.0.

### 3.3. Simulation Assumptions

In BACKSCAT, the lidar transmit beam is assumed to be collimated and there is no focusing. The transmit and receive optics/beams are collinear which is a monostatic system with no optics offsets. The local oscillator power is assumed to be large enough such that the system is shot noise limited with the SNR dominated by the local oscillator noise source.

In this preliminary study there are no turbulence or speckle effects included which can degrade the beam and reduce the return signal. The local oscillator and receive beam phase fronts are assumed to be matched so that there are no phasing losses.

### 3.4. Equations in BACKSCAT 4.0

The voltage signal-to-noise ( $\text{SNR}_v$ ), is calculated for a single pulse as

$$\text{SNR}_v = \sqrt{\frac{\eta P_s}{h\nu BF}}, \quad (3)$$

where  $P_s$  is the return power into the receiver,  $\eta$  is the detector's quantum efficiency,  $h$  is Planck constant,  $\nu$  is the laser frequency ( $= c/\lambda$ ),  $c$  is the speed of light,  $F$  is the detector excess noise factor, and  $B$  is the bandwidth of the receiver electronics assumed to be a matched filter.

The return signal power is defined as

$$\begin{aligned} P_s &= E_p \tau_T \tau_R \tau_w^2 \tau_a^2 \frac{\beta c}{2} \frac{A_R}{R^2} \\ &= 1.63 \times 10^{-4} \frac{\beta \tau_a^2}{R_{\text{km}}^2}, \end{aligned} \quad (4)$$

where  $\beta$  is the aerosol backscatter coefficient in  $\text{m}^{-1} \text{sr}^{-1}$ ,  $A_R$  is the receiver collector area,  $\tau_a$  is the one-way atmospheric transmission,  $\tau_T$  is the transmitter optical transmission,  $\tau_R$  is the receiver optical transmission,  $\tau_w$  is the one-way transmission through the quartz window on the aircraft, and  $R$  is the range from the aircraft to a given altitude at the specific viewing angles of the lidar.

Substituting in for the lidar system parameters, the  $\text{SNR}_v$  becomes,

$$\begin{aligned} \text{SNR}_v &= 1.61 \times 10^6 \sqrt{P_s}, \\ &= 2.04 \times 10^4 \frac{\sqrt{\beta} \tau_a}{R_{\text{km}}}, \end{aligned} \quad (5)$$

In the SNR relation, it is assumed that a matched filter is used in the detector electronics, *i.e.*,

$$B = \frac{1}{2t_p}. \quad (6)$$

## 4. SNR PERFORMANCE PREDICTIONS

### 4.1. Single Pulse Operation

BACKSCAT runs were made to predict the various effects that can influence the single pulse operation of the Ballistic Winds lidar. These results are shown in Figures 12 through 15 where the molecular effects, the viewing angle, the aircraft altitude, and the laser lines were individually varied. In all of these calculations, molecular backscatter is not included in the signal return, except for the investigation of the various molecular effects (Figure 12).

The trends in each case are similar, the voltage SNR is relatively large near the aircraft, enough for single pulse detection of the return. The signal decreases due to the increasing range with insufficient backscatter to compensate for the range losses until near the boundary layer. Although the aerosol return is largest in the boundary layer, this region does not affect the ballistic trajectory and the returns from this region would not be processed in any operational system. When all the various scenarios analyzed are compared, there is not a great variation in the resultant SNR.

This indistinguishable results in Figure 15 are especially important for the laser line SNR predictions. That is, the Lightwave Laser system is not able to tune itself to the peak of the molecular transmission line, but the effect of being "off peak" is unimportant.

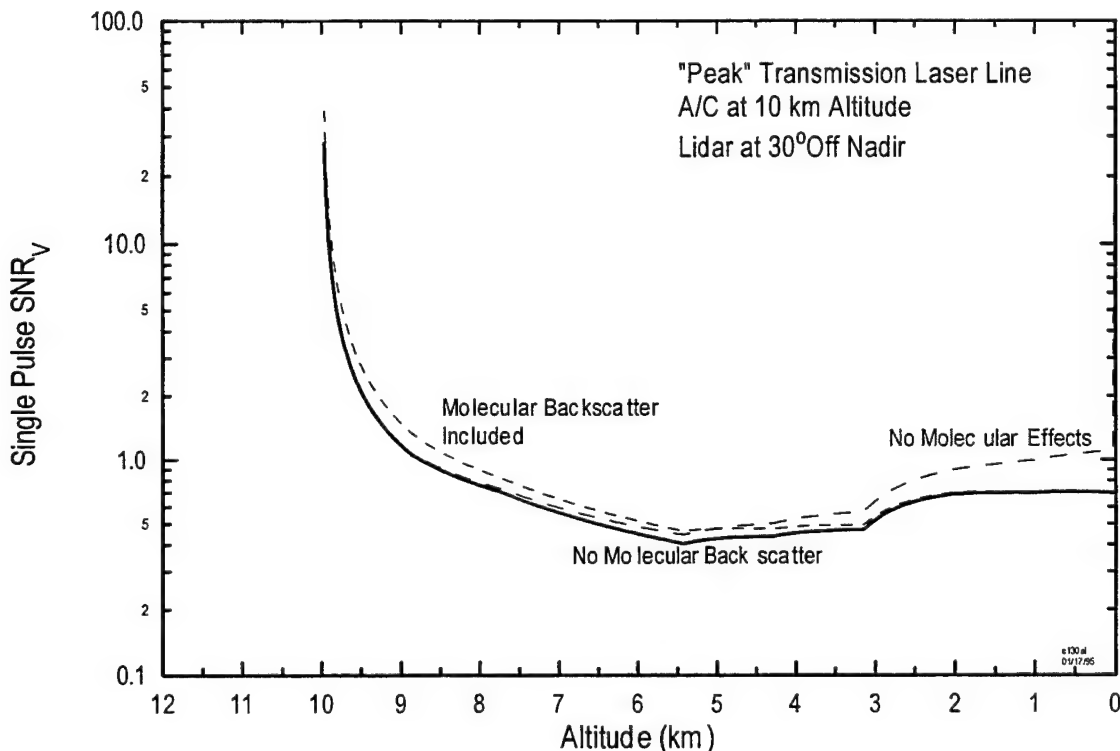


Figure 12. Molecular attenuation variation effects on BACKSCAT single pulse SNR.

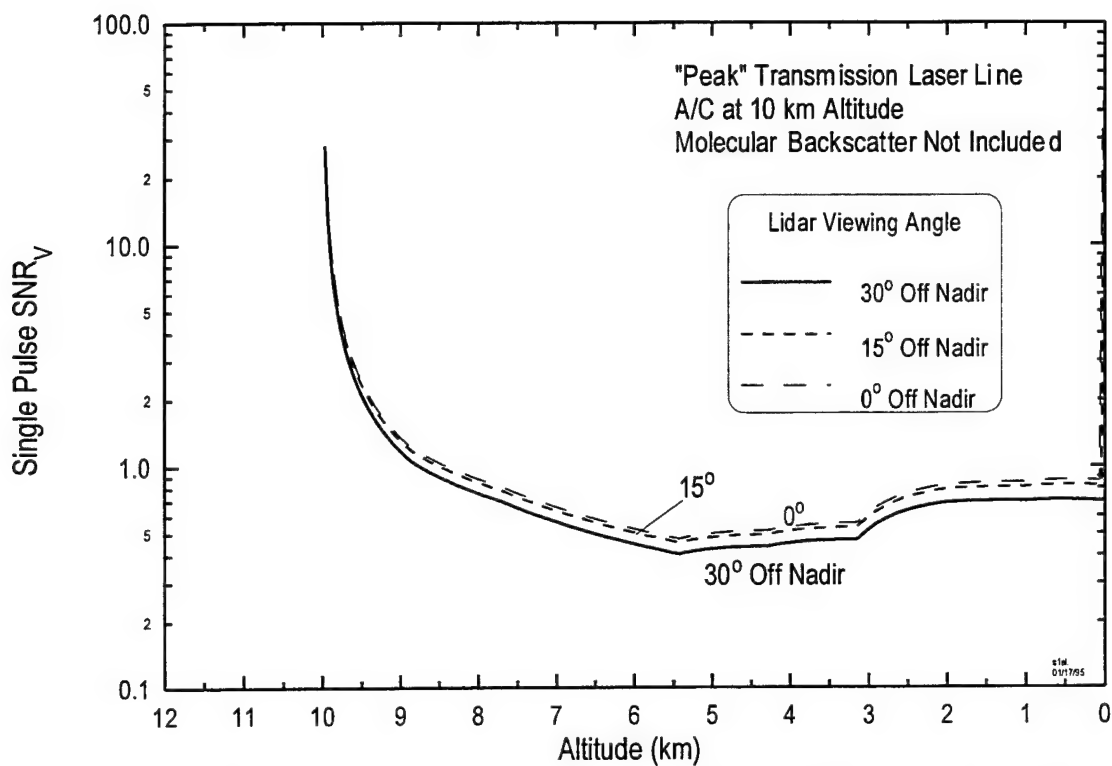


Figure 13. Viewing angle variation effects on BACKSCAT single pulse SNR.

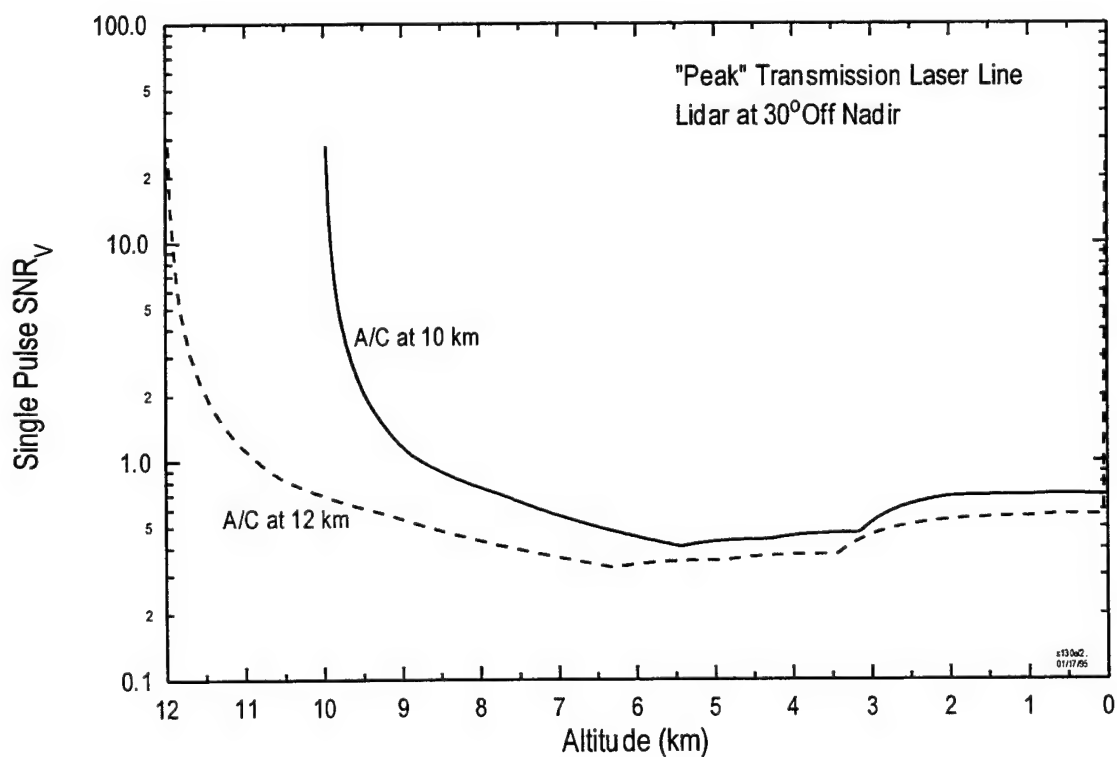


Figure 14. Aircraft altitude variation effects on BACKSCAT single pulse SNR.

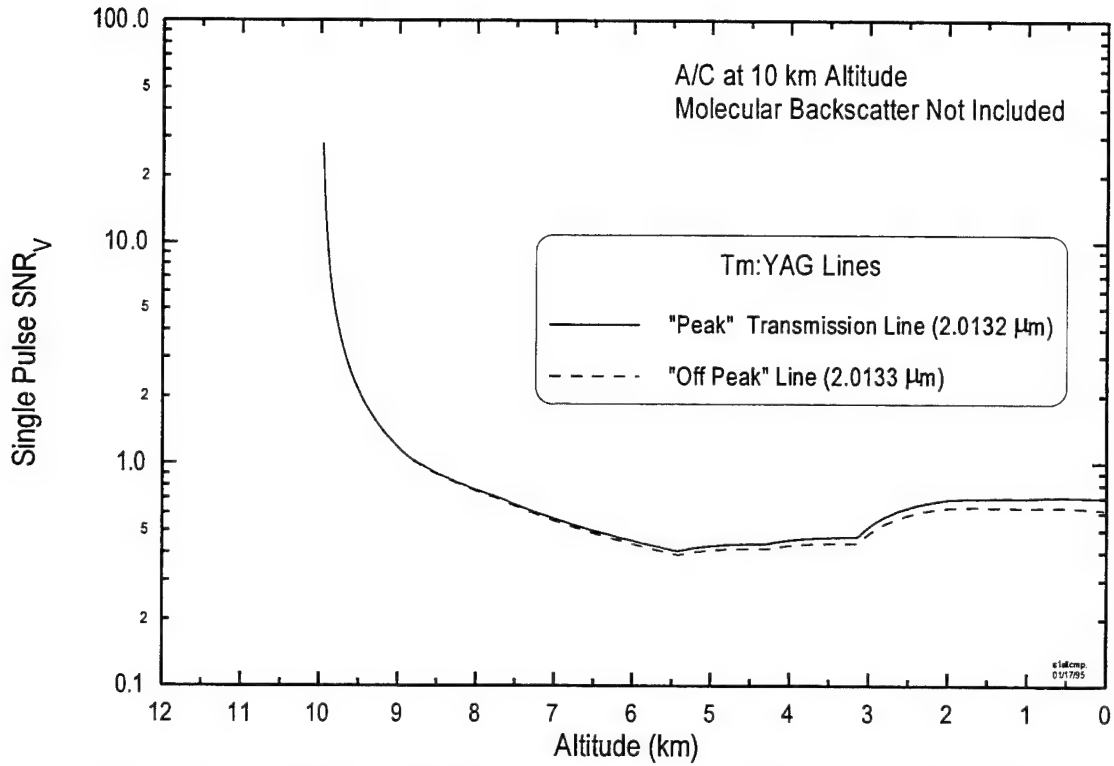


Figure 15. Laser line variation effects on BACKSCAT single pulse SNR.

#### 4.2. Pulse Integration Performance

Pulse integration can increase the signal-to-noise by summing single pulses such that the return signal power is increased at a faster rate than that of the noise power. Ideal pulse also called coherent integration, increases the resultant SNR by the number of pulses summed. In incoherent, or post detection integration, the signal-to-noise is increased by the square root of the number of pulses summed. With most pulse integration processes, the integrated signal-to-noise ( $SNR_i$ ) falls between coherent pulse integration with a gain ( $\gamma$ ) of one and post detection integration with a gain of 0.5, *i.e.*,

$$SNR_i = N^\gamma SNR_1 \quad (0.5 \leq \gamma \leq 1). \quad (7)$$

where  $N$  is the number of pulses summed and  $SNR_1$  is the single pulse signal-to-noise ratio.

There are many factor which affect the integration efficiency. These include the number of pulses summed, the receiver electronics, the target characteristics, and the pulse timing, shape, *etc.* As a worst case, it is assumed that the ballistic winds pulse summing process is incoherent ( $\gamma = 0.5$ ).

When summing the lidar return pulses, it is assumed that the wind field remains uniform and constant over the number of pulses required to reach the desired integrated SNR. The time limitations to this assumption will have to be determined during the field tests.

In the following analysis, it is assumed that 10 dB power SNR is required for wind field detection in each range bin. This SNR (power) is equivalent to a SNR (voltage) of 5 dB (equivalent to a ratio of 3.2). Figures 16 through 19 show the required number of integrated pulses necessary to reach this total return power. The figures are in the same order as the single pulse SNR figures shown previously. For an aircraft flying at 10 km, the maximum number of pulses that must be summed to maintain 10 dB signal-to-noise (power) is 64. This occurs in approximately the 5.5 km altitude region.

Figure 20 shows the required number of pulses that must be summed to maintain a desired integrated SNR while the various molecular effects are accounted for. This is for an aircraft cruising at 10 km altitude using the "peak" laser line.

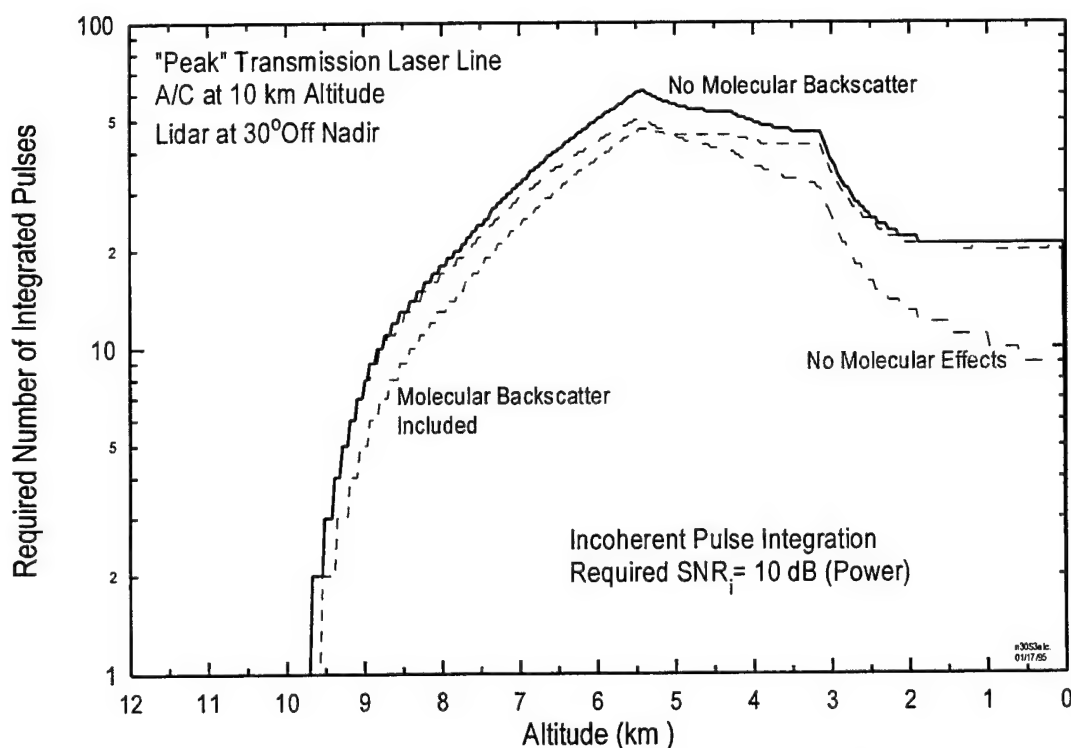


Figure 16. Molecular effects variation on the required number of integrated pulses.

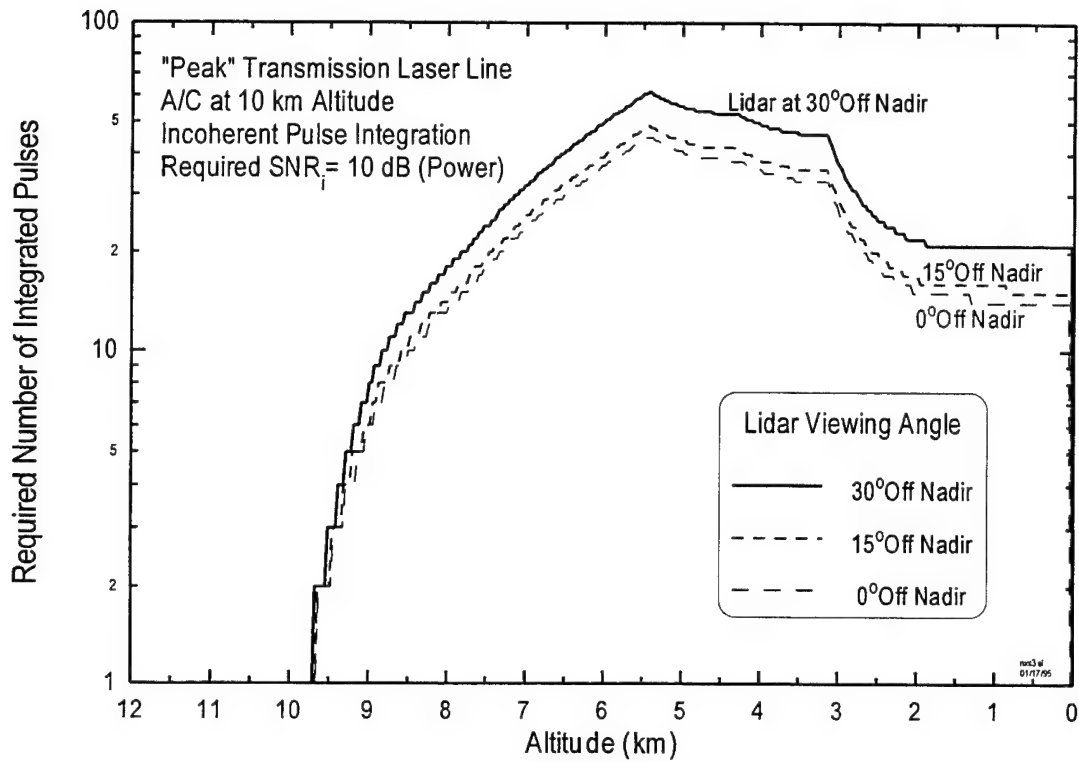


Figure 17. Viewing angle variation effects on the required number of integrated pulses.

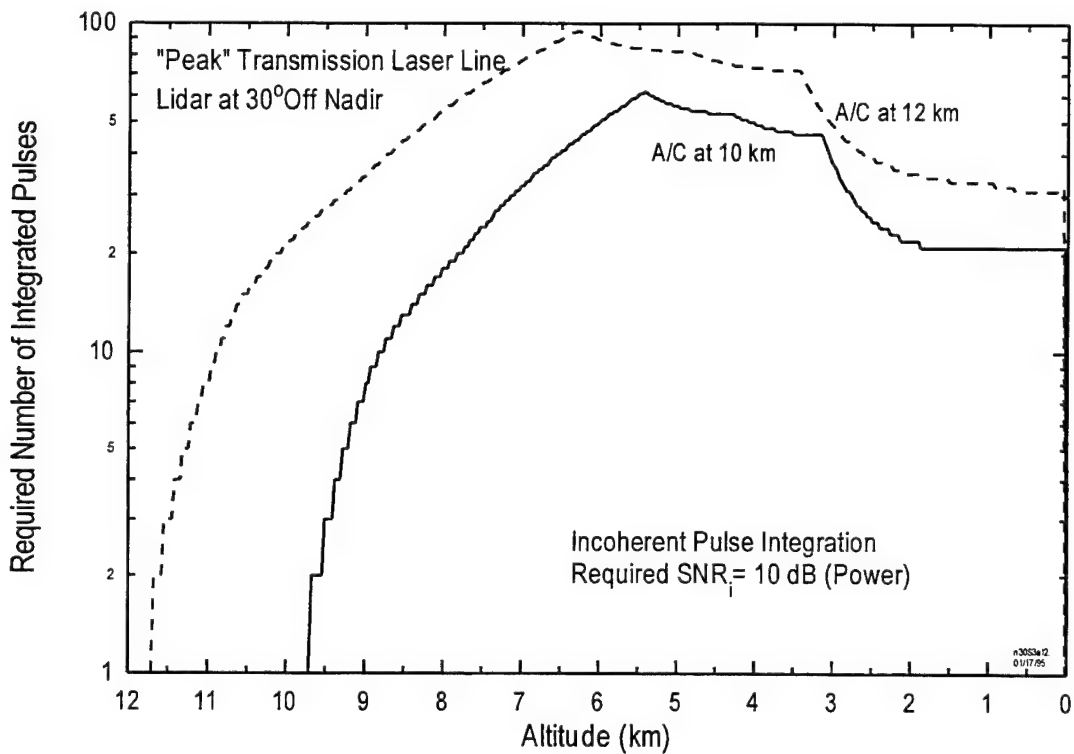


Figure 18. Aircraft altitude variation effects on the required number of integrated pulses.

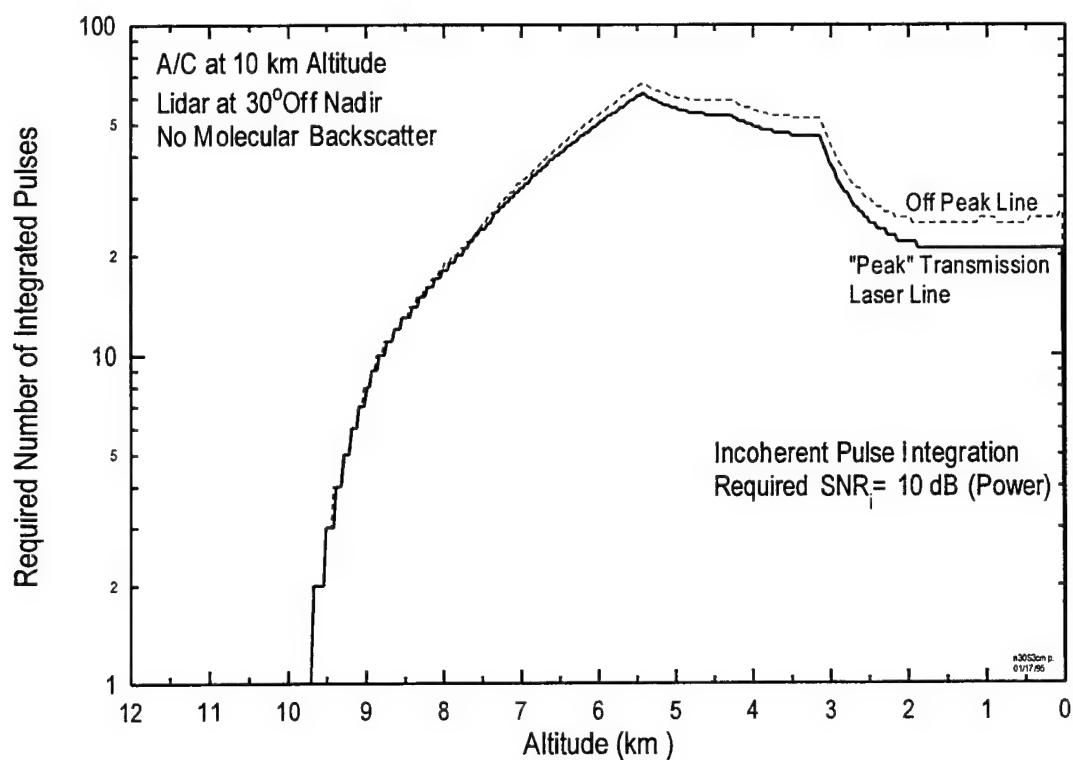


Figure 19. Laser line variation effects on the required number of integrated pulses.

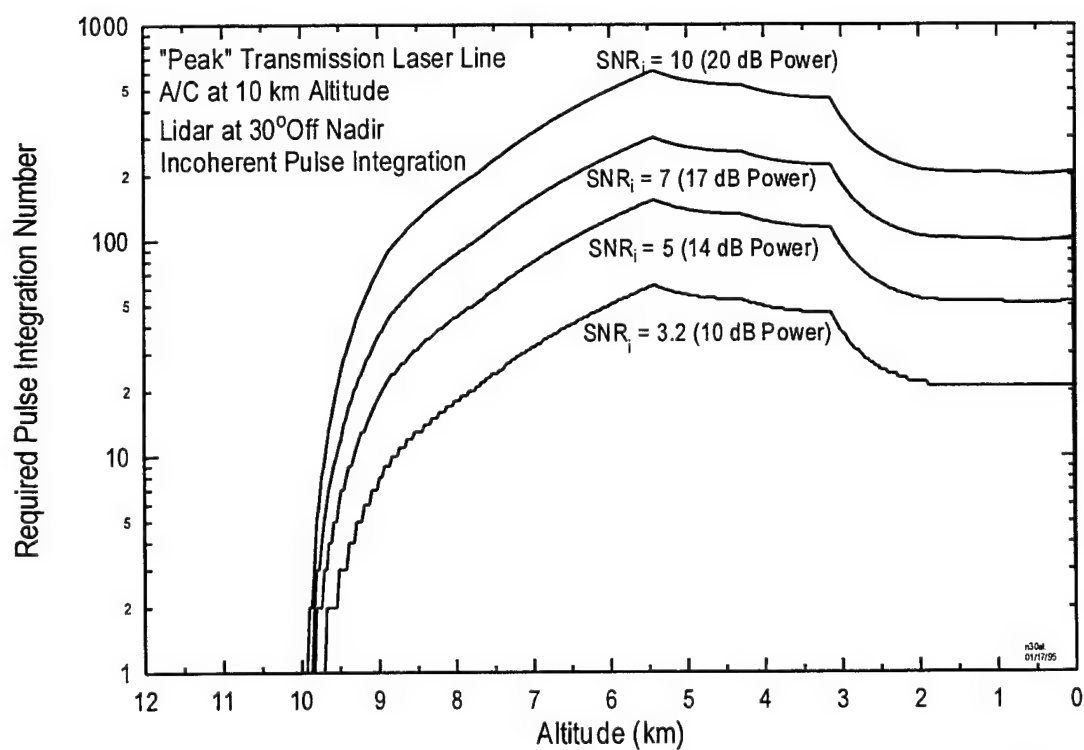


Figure 20. Required number of integrated pulses to maintain a desired total SNR.



### 4.3. Range and Velocity Resolution Considerations

Range and velocity resolutions for a pulsed Doppler lidar system are inversely related. If improved velocity resolution (and accuracy) is desired, then there is a sacrifice in the range resolution (and accuracy).

The maximum range resolution,  $\Delta R$ , is

$$\Delta R = \frac{c t_p}{2}. \quad (8)$$

where  $t_p$  is the laser pulse length. The velocity resolution,  $\Delta V$ , is

$$\Delta V = \frac{\lambda \Delta f}{2} = \frac{\lambda}{2 t_p}, \quad (9)$$

where  $\Delta f$  is the I.F. (intermediate frequency) Doppler shift due to the change in line-of-sight velocity,

$$\Delta f = \frac{2 V_{LOS}}{\lambda}. \quad (10)$$

This leads to the relationship between the velocity and range resolution; that their product is a constant dependent only upon the lidar wavelength,

$$\Delta R \Delta V = \frac{c \lambda}{4}. \quad (11)$$

For the present Ballistic Winds coherent lidar, the constant product ( $\Delta R \Delta V$ ) has a value of 151 m<sup>2</sup>/s. With a BW laser pulse length of 0.25  $\mu$ s, the maximum range resolution is 37.5m and the velocity resolution is 4 m/s.

### 4.4. Velocity Accuracy Considerations

The velocity accuracy,  $\sigma_V$ , which is related to the Doppler frequency accuracy ( $\sigma_f$ ), is dependent on the SNR<sub>V</sub><sup>7</sup>,

---

<sup>7</sup> Skolnik, M.I., editor (1970) *Radar Handbook*, McGraw-Hill, New York.

$$\begin{aligned}\sigma_v &= \frac{\lambda}{2} \sigma_f \\ &= \sqrt{\frac{3}{2}} \frac{1}{2\pi} \frac{\lambda}{t_p \text{SNR}_v},\end{aligned}\tag{12}$$

Using  $t_p$  for the BW lidar, the relationship in Eq. (12) is illustrated in Figure 21. The single hit velocity accuracy for the BW simulation is shown in Figure 22 for different viewing angles. Once again, molecular backscatter effects are not included in the return signal. The curve in this figure is just the mirror image of the single pulse SNR curves since the accuracy for fixed pulse length depends only on the inverse of the SNR.

When pulse summing is used to increase SNR, the effective velocity accuracy reaches a plateau that depends on the required integrated SNR. There are negligible variations in the integrated accuracy from the various lidar parameter variations analyzed. Figure 23 shows the integrated pulse velocity accuracy with viewing angle variations analyzed. The velocity accuracy reaches about 0.5 m/s (for 10 dB power) by 9 km altitude.

To further establish the validity of the statement that the velocity accuracy only improves as  $N^{1/2}$  for the Ballistic Winds coherent lidar, the analysis of Dunn<sup>8</sup> was utilized. Dunn gives the lower bounds on velocity estimation using single hit accuracy/resolution with polynomial smoothing and centered data intervals as,

$$\sigma_v^2 = \left[ \left[ \frac{\Delta V^2}{N} \right]^{-1} + \left[ \frac{12 \Delta R^2 v^2}{N(N^2 - 1)} \right]^{-1} \right]^{-1},\tag{13}$$

where  $v$  is the laser PRF. For the BW lidar system values give, the improvement in velocity accuracy varies as  $N^{1/2}$  for the BW WSMR lidar system, as expected for incoherent pulse summation. The first term in Eq. (13) dominates since  $(\Delta R v)^2$  is much larger than  $(\Delta V)^2$ . This relation is plotted in Figure 24.

---

<sup>8</sup> Dunn, K.-P. (1987) *Lower Bounds on Acceleration Estimation Accuracy*, MIT Lincoln Laboratory, Technical Report #790, ESD-TR-87-080, 5 October, ADA18838314.

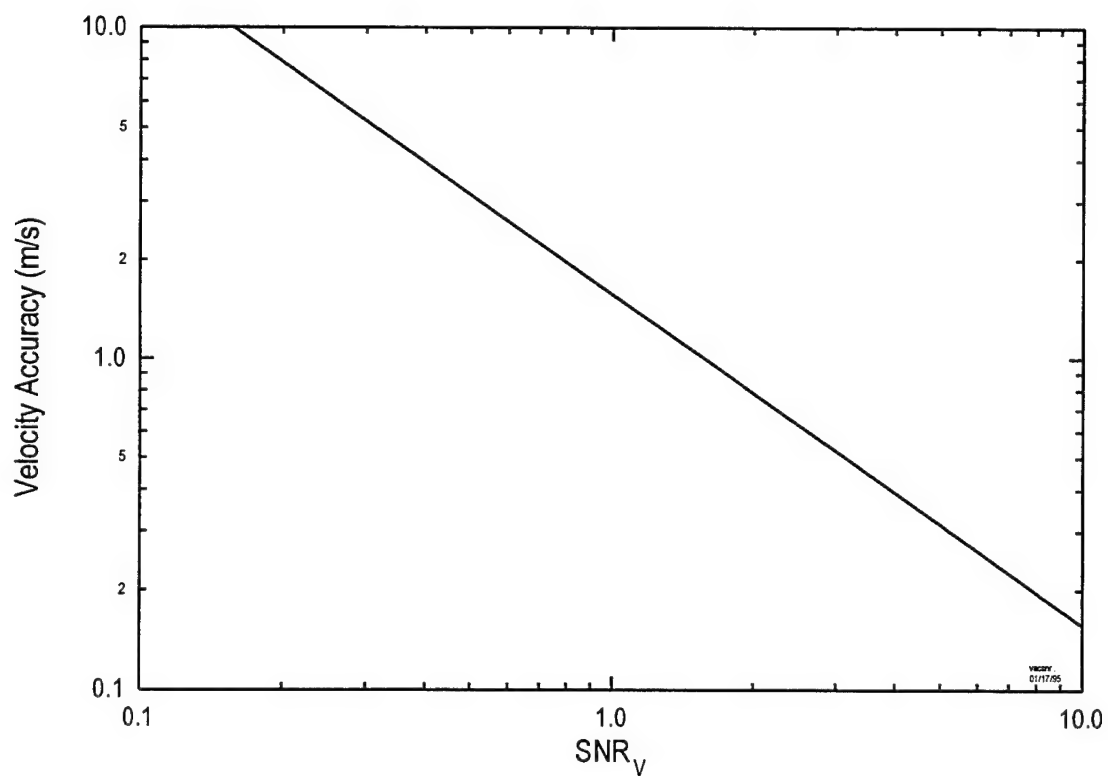


Figure 21. Velocity accuracy vs. voltage SNR.

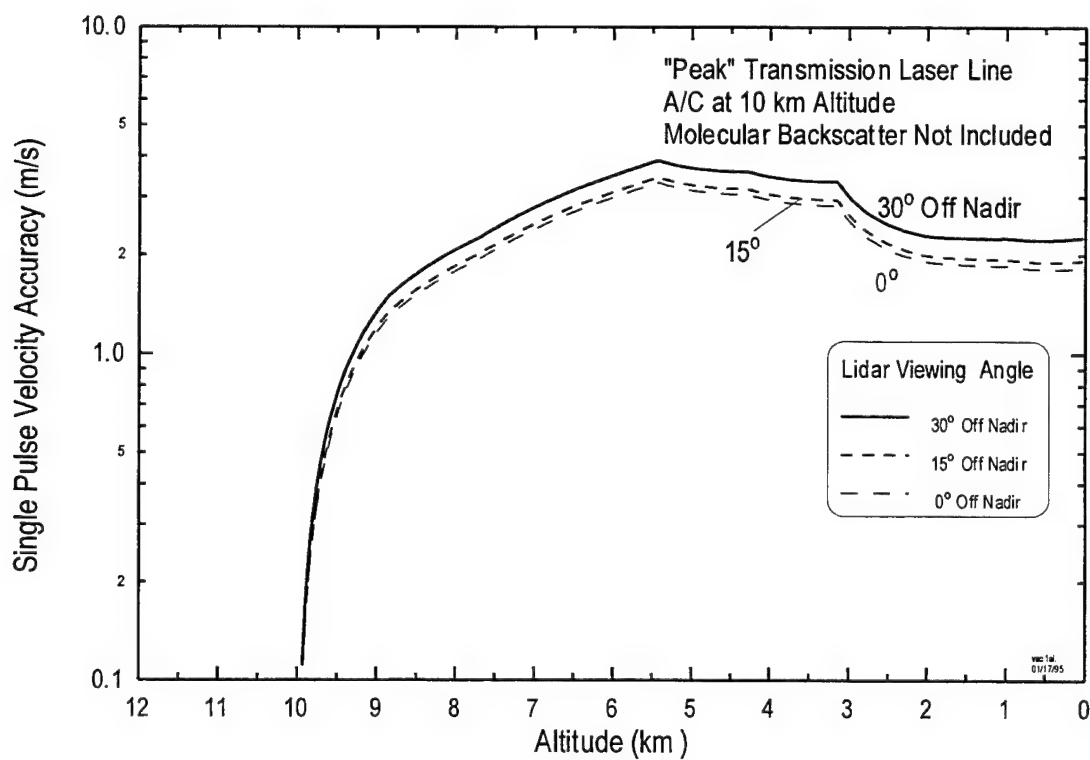


Figure 22. Viewing angle variation effects on the single hit velocity accuracy.

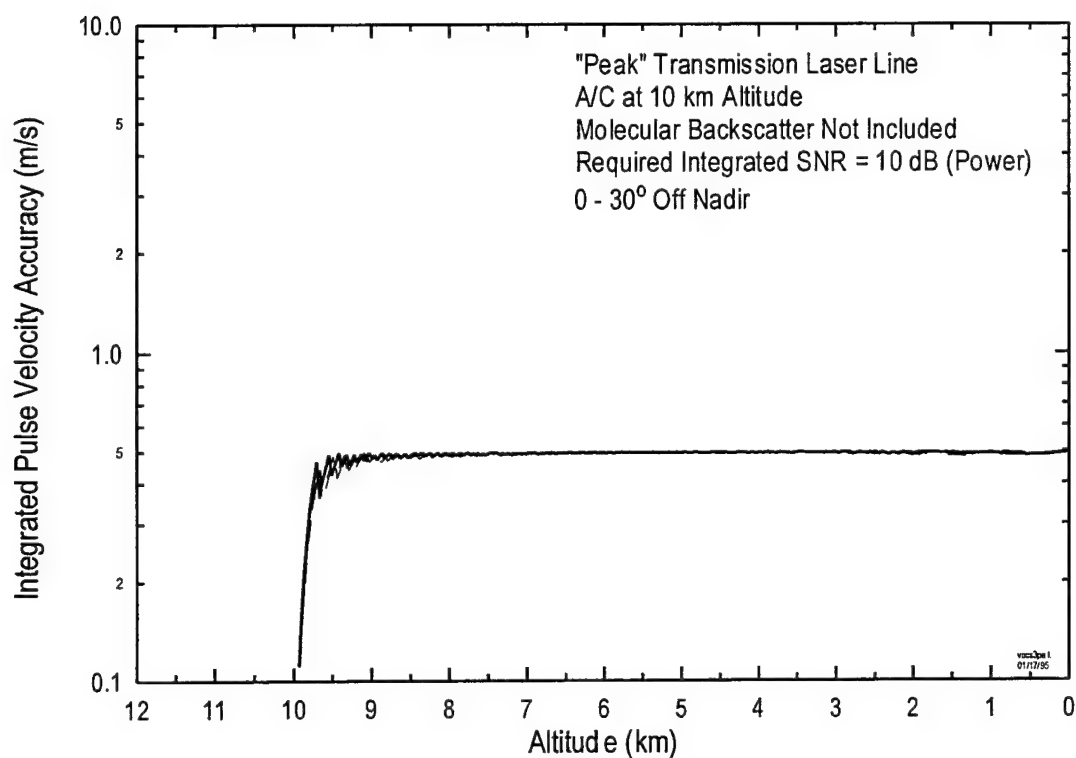


Figure 23. Integrated pulse velocity accuracy vs. altitude.

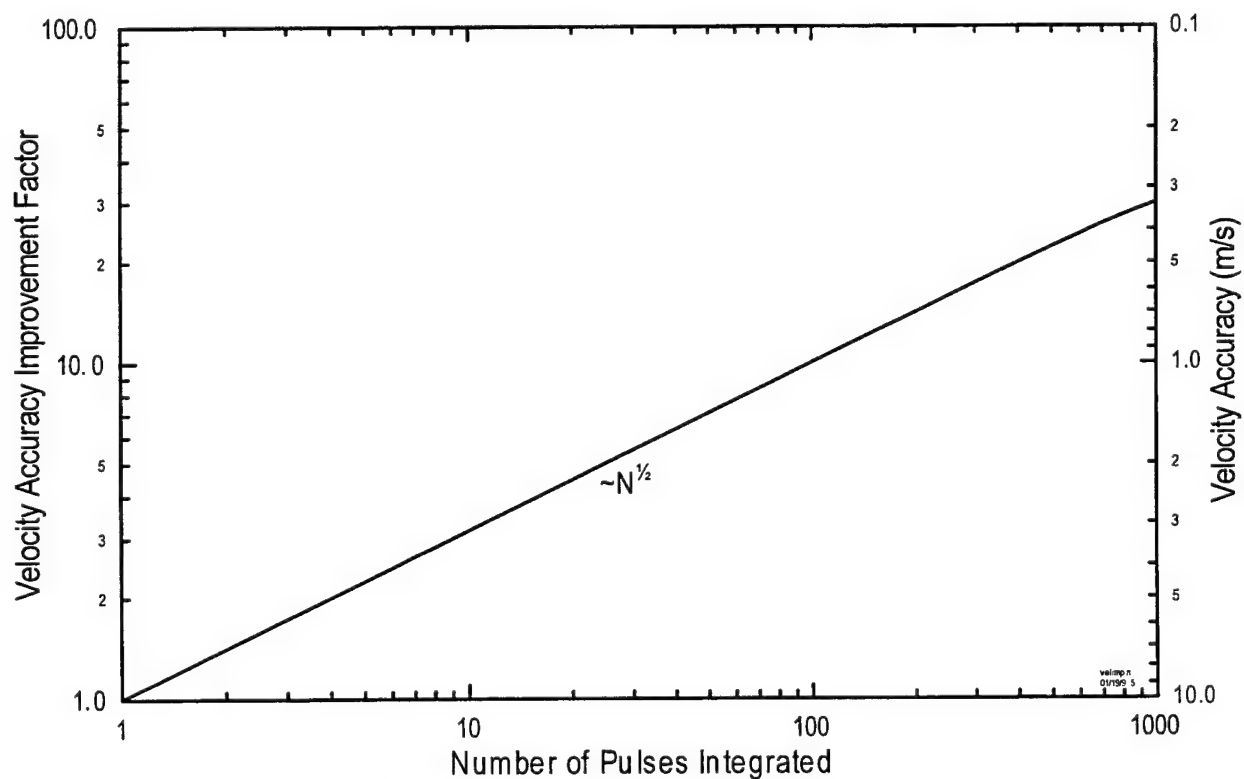


Figure 24. Velocity estimation accuracy for BW Doppler lidar.

## 5. WIND EFFECTS ON AIRCRAFT

This section describes the effects of the crosswind on the operation of the Doppler lidar and how the results of the tests must take this into account. During the final leg of the racetrack pattern flown by the B-52, the aircraft is flying orthogonal to the prevailing WSMR westerly winds. In order to fly due north during the bomb run, the pilot must fly slightly into the crosswind ( $V_W$ ) to maintain his course as shown in Figure 25. This heading angle into the wind ( $\theta_h$ ), depends on the aircraft velocity ( $V_{A/C}$ ) as,

$$\theta_h = \sin^{-1}(V_W / V_{A/C}), \quad (14)$$

where the effective A/C ground velocity ( $V_{eff}$ ) is,

$$\begin{aligned} V_{eff} &= V_{A/C} \cos \theta_h \\ &= \sqrt{V_{A/C}^2 - V_W^2}. \end{aligned} \quad (15)$$

This heading angle correction for the final leg is shown in Figure 26 for the two expected extremes of the aircraft's velocity. The heading angle correction for the prevailing crosswind is between  $10^\circ$  and  $15^\circ$ .

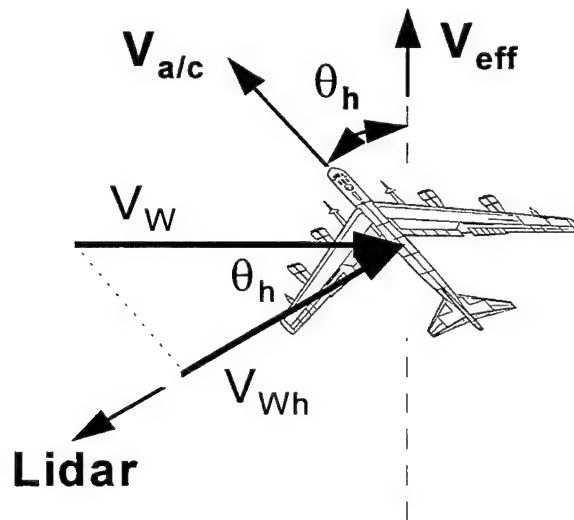


Figure 25. Aircraft orientation during bomb drop test leg.

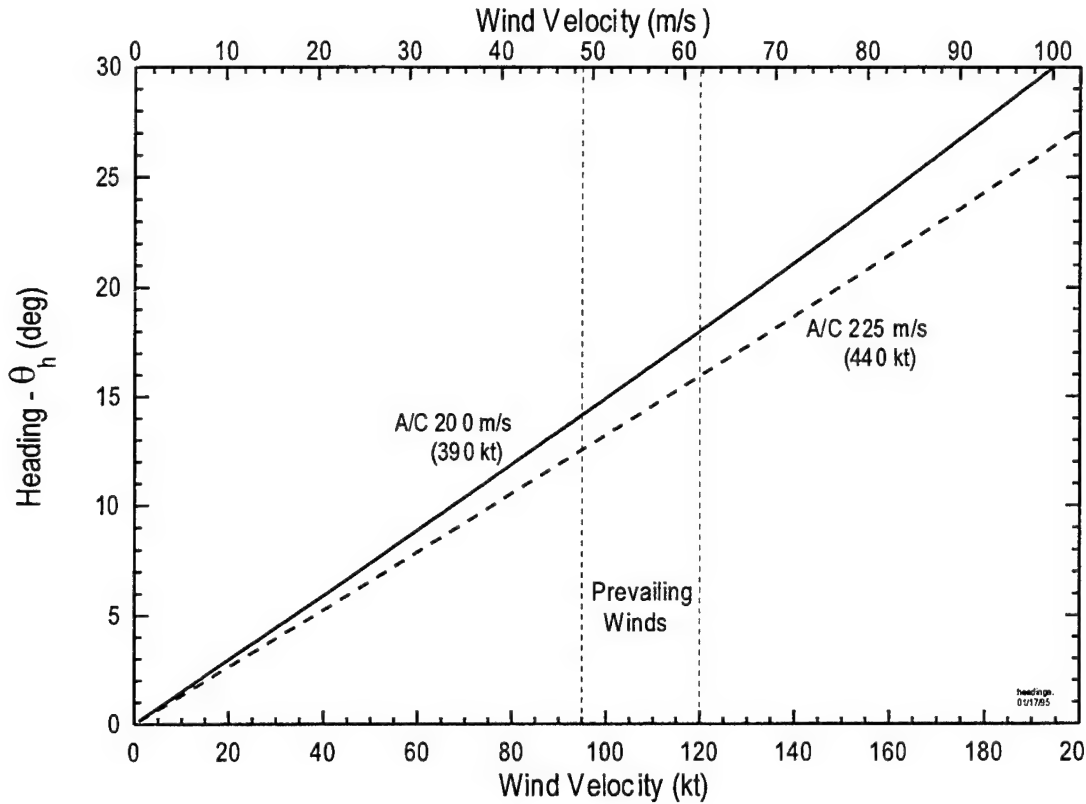


Figure 26. Aircraft heading vs. wind velocity.

The heading into the wind affects the Doppler lidar wind measurements. Given that the lidar's line-of-sight is always orthogonal to the A/C velocity vector, the LOS wind velocity ( $V_{Wh_{LOS}}$ ) as measured by the lidar is,

$$\begin{aligned} V_{Wh_{LOS}} &= V_{Wh} \sin \phi_N \\ &= V_W \cos \theta_h \sin \phi_N. \end{aligned} \quad (16)$$

Eq. (16) includes the effects of the off nadir viewing angle ( $\phi_N$ ) as illustrated in Figure 27.

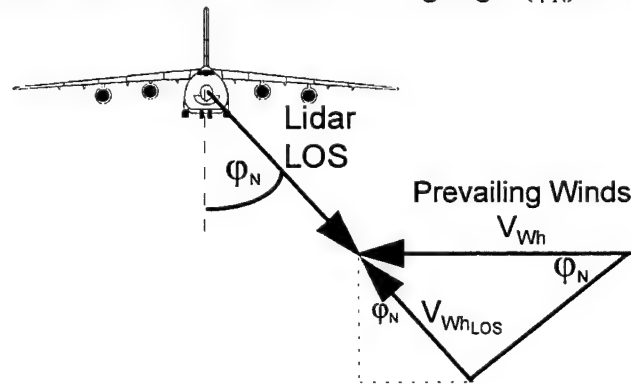


Figure 27. Off nadir viewing angle effect on LOS wind vector.

The relative LOS velocity reduction with no nadir effects included ( $\phi_N = 90^\circ$ ) is illustrated in Figure 29. This loss due to the A/C heading into the wind to maintain course, is less than a 4% effect and is not a cause for concern.

When the off nadir viewing angle is included, the normalized LOS horizontal wind component measured is further reduced by the sine of the off nadir angle. This further reduction is shown in Figure 29. A  $15^\circ$  off nadir angle reduces the measured horizontal wind component to 26% of its value. Depending on the magnitude of the prevailing winds, this can reduce the velocity measurement to within the velocity resolution limit, resulting in incorrectly converting to the horizontal wind speed. Increasing the off nadir angle to  $30^\circ$  almost doubles the required components measured value.

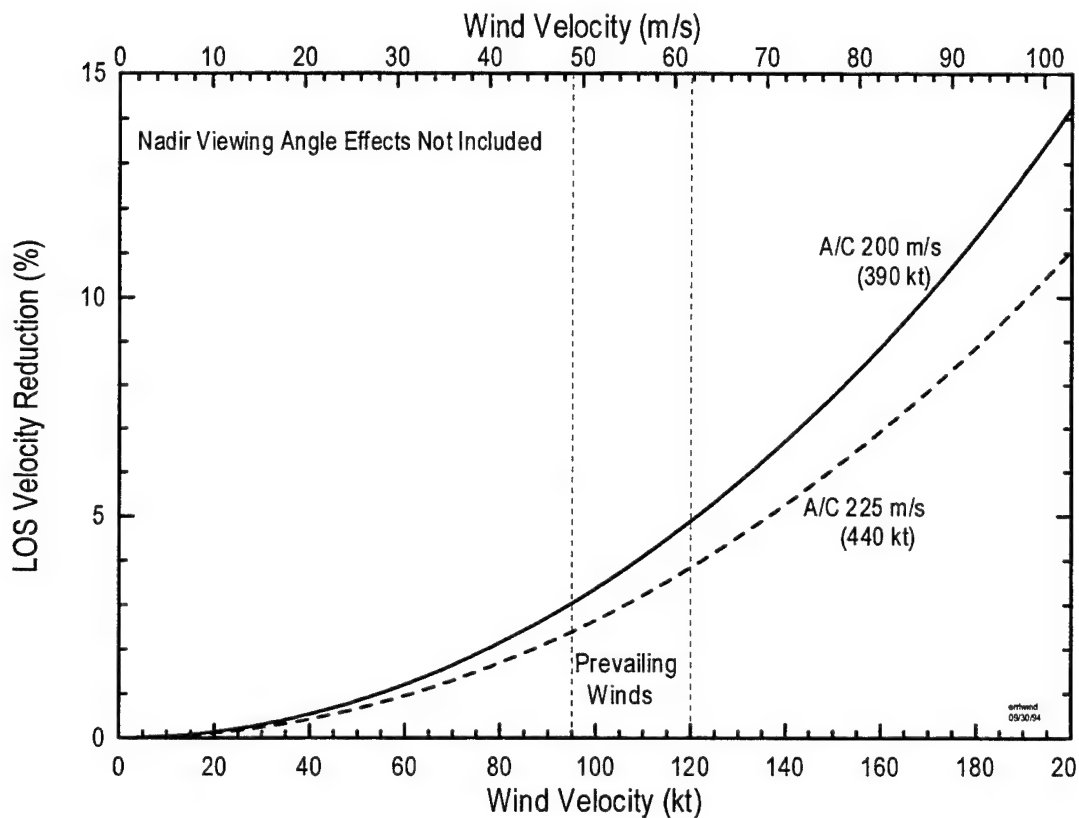


Figure 28. LOS velocity reduction due to crosswind.

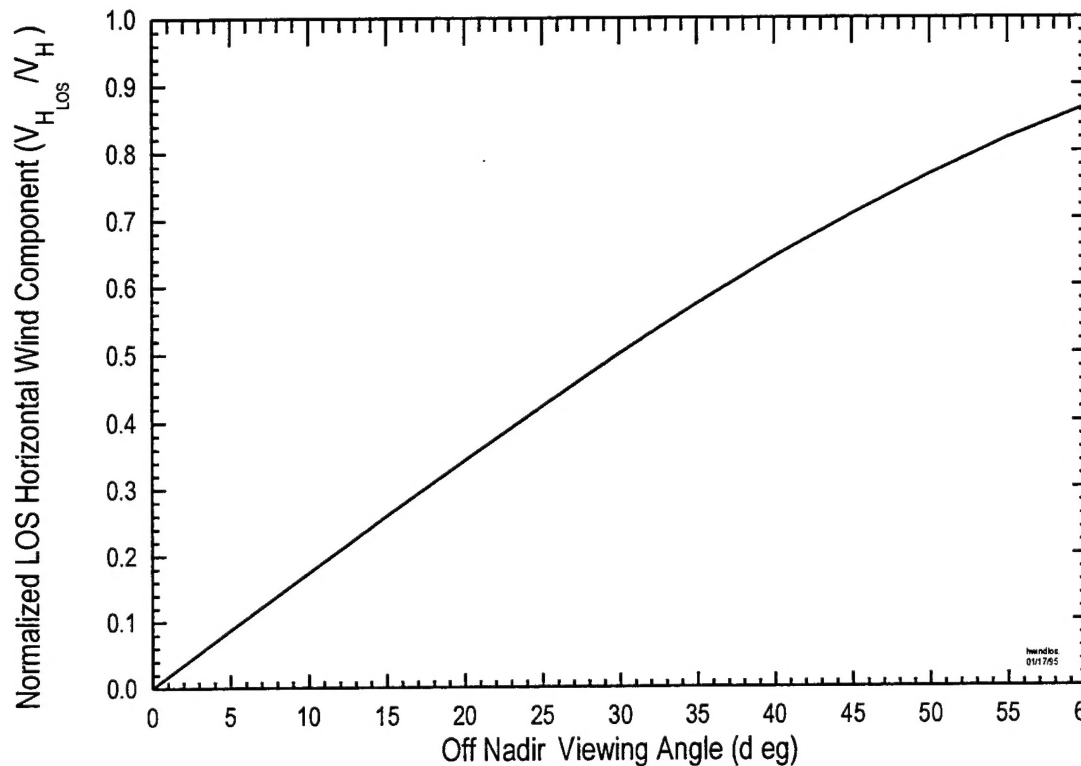


Figure 29. Relative LOS horizontal wind component due to lidar off nadir angle.

## 6. SUMMARY AND CONCLUSIONS

This study gives a methodology for predicting the performance of coherent lidar systems which use the atmospheric background aerosols as a backscattering medium to obtain a measurement signal. A real time, high altitude wind profile can be obtained and used by onboard aircraft targeting systems utilizing coherent Doppler lidars to make more refined ballistic wind corrections.

The major conclusion of this preliminary study on the current Ballistic Winds Doppler lidar is that the system, with pulse summing techniques, is feasible and can make the necessary measurements during aircraft flights at White Sands or elsewhere. Although the present analysis showed that summing less than 100 pulses can measure the high altitude winds, there is one major caveat. That is, this study used the "nominal" atmospheric conditions and constituents contained in the LOWTRAN7 model, and no real atmosphere is ever "nominal". Experience at the Utah Test and Training Range<sup>9</sup> has shown that there are days when there are not enough aerosols present to obtain measurements back from even a powerful ground based CO<sub>2</sub> coherent lidar let alone a small aircraft-based lidar system. Experimental results have shown that the LOWTRAN aerosol models' loadings, at least at high altitude, give larger, more optimistic

<sup>9</sup> Beland, R.R. (1995) Private Communication, Air Force Phillips Laboratory/Geophysics Directorate (PL/GPOA), Hanscom AFB, MA.



signal returns. More pulse summing will probably be necessary in order to obtain reliable signal levels from actual measurements programs.

There are many methods available to increase the signal return into the detector. The most obvious is to increase the transmitted pulse energy, but this is not always possible since most new applications are pushing the state-of-the-art and increased energy is difficult to come by. Other improvement techniques are to increase the number of pulses summed, improve the optics efficiency, operate at a different wavelength with more backscattering and less attenuation, obtain a more efficient detector/optics coupling, increase the off nadir look angle, *etc.* Each of these applications has problems associated with its implementation.

One of the easiest methods to increase the single pulse SNR and avoid the difficulty of pulse summing is to increase the size of the collection aperture. There is a one-to-one increase in improvement with the increase in receiver diameter. This is shown in Figure 30 where the 7 cm collector is assumed to be the baseline design. Increasing the receiver aperture from 7 cm to 10 cm, the required pulse integration factor would decrease by 1.4.

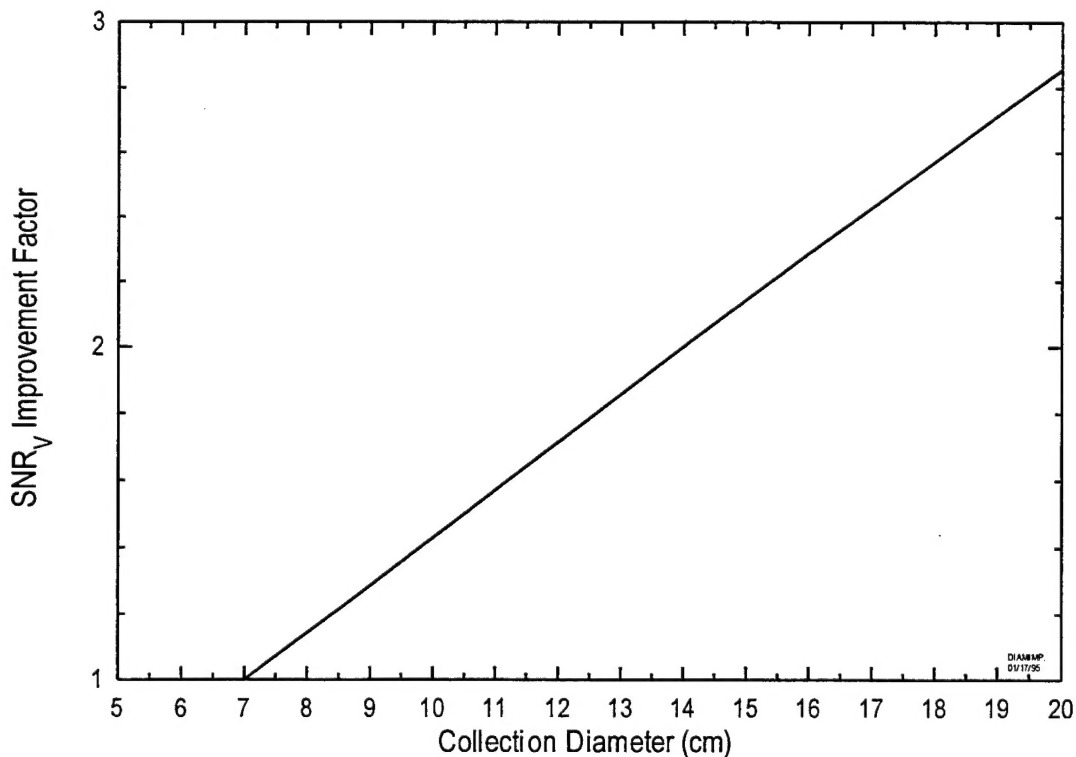


Figure 30. SNR improvement factor vs. collection aperture size.

Although the system will be initially installed on a B-52 at an off nadir viewing angle of 15° which is the maximum angle due to optics and space limitations, this angle is far from optimum for wind measurements. The off nadir viewing angle should be as large as possible, consistent with meeting the requirements for measuring the wind at the desired minimum

altitude. An angle of at least  $30^\circ$  would increase the horizontal wind component measurement by a factor of two.

Molecular absorption is important, but maintaining the laser wavelength tuned near the peak of a transmission line is relatively easy. Furthermore, most absorption lines are broad enough to have a relatively small effect on the laser's transmission.

It cannot be emphasized enough that these analyses were made with LOWTRAN7 standard mid-latitude spring/summer atmospheric profiles. The real atmosphere can be (and usually is) appreciably different - orders of magnitude variation in attenuation and scatter coefficients compared to "nominal" are not uncommon. This leads to the open question of what the aerosol concentration at the high altitudes, especially the tropopause, really is at the sites of interest. The tropopause is a highly variable region and can greatly affect the SNR and pulse summing predictions. For any reliable predictions of field test results, actual atmospheric profiles especially those relating directly to the laser backscatter coefficient should be measured at the site.

## 7. REFERENCES

1. Kneizys, F.X. Shettle, E.P., Abreu, L.W., Chetwynd, J.H., Anderson, G.P., Gallery, W.O., Selby, J.E.A., and Clough, S.A. (1988) *Users Guide to LOWTRAN7*, Air Force Geophysics Laboratory, Hanscom AFB, MA, AFGL-TR-88-0177, ADA 206773.
2. Jenne, R.L. (1994) *Jenne's Northern Hemisphere Climatology - Monthly (1950 - 1964) Data Set DS205.0*, NCAR Research Data Archives, Available over the Internet (<ftp://ncardata.ucar.edu/datasets/ds205.0>).
3. Anderson, G.P., Chetwynd, J.H. (1993) "Fast Atmospheric Signature Code Version 3 - Preliminary", Presented at The Joint Phillips - Wright Laboratories Atmospheric Propagation Workshop, Wright-Patterson AFB, OH, 18 - 20 May, Handout #8.
4. Fenn, R.W., Clough, S.A., Gallery, W.O., Goode, R.E., Kneizys, F.X., Mill, J.D., Rothman, L.S., Shettle, E.P., and Volz, F.E. (1985) "Optical and Infrared Properties of the Atmosphere", Chap 18 in *Handbook of Geophysics and the Space Environment*, A.S. Jursa (Scientific Editor), Air Force Geophysics Laboratory, Hanscom AFB, MA, AFGL-TR-85-0315, ADA 167000.
5. Moody, S.E. (1987) "Evaluation of Laser Technologies for On-Aircraft Wind Shear Detection," SPIE Vol. 783, p.124.
6. Longtin, D.R., Cheifetz, M.G., Jones, J.R., and Hummel, J.R. (1994) *BACKSCAT Lidar Simulation Version 4.0: Technical Documentation and Users Guide*, Phillips Laboratory, Directorate of Geophysics, Hanscom AFB, MA, PL-TR-94-2170, ADA285851.
7. Skolnik, M.I. editor (1970) *Radar Handbook*, McGraw-Hill, New York.
8. Dunn, K.-P. (1987) Lower Bounds on Acceleration Estimation Accuracy, MIT Lincoln Laboratory, Technical Report #790, ESD-TR-87-080, 5 October, ADA18838314.
9. Beland, R.R. (1995) Private Communication, Air Force Phillips Laboratory/Geophysics Directorate (PL/GPOA), Hanscom AFB, MA.